From Diffractive QCD to the Observation of ZZ Production

Michael Strang

State University of New York, Buffalo

Outline

- Work as a grad student
  - Diffractive QCD
  - Forward Proton Detector

- Work as a post doc
  - CMS
    - Work on Simulation Validation
    - Work on Automated Software Flow for Data Quality Monitoring
  - DØ
    - Measurement of ZZ Production in 4 lepton channel

DØ diffraction and dijet evidence with the Forward Proton Detector

Typical QCD Event

- In a proton-antiproton collision, a quark or gluon can be exchanged:

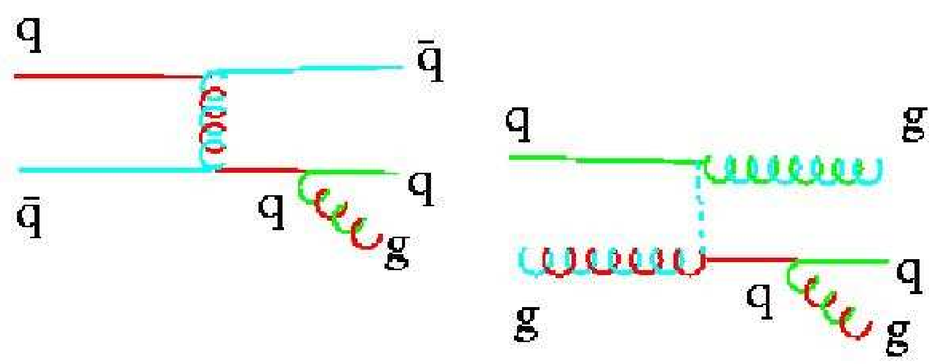

- Due to the color flow in the event, particles are produced throughout phase space and concentrated in regions around the struck partons (jets)

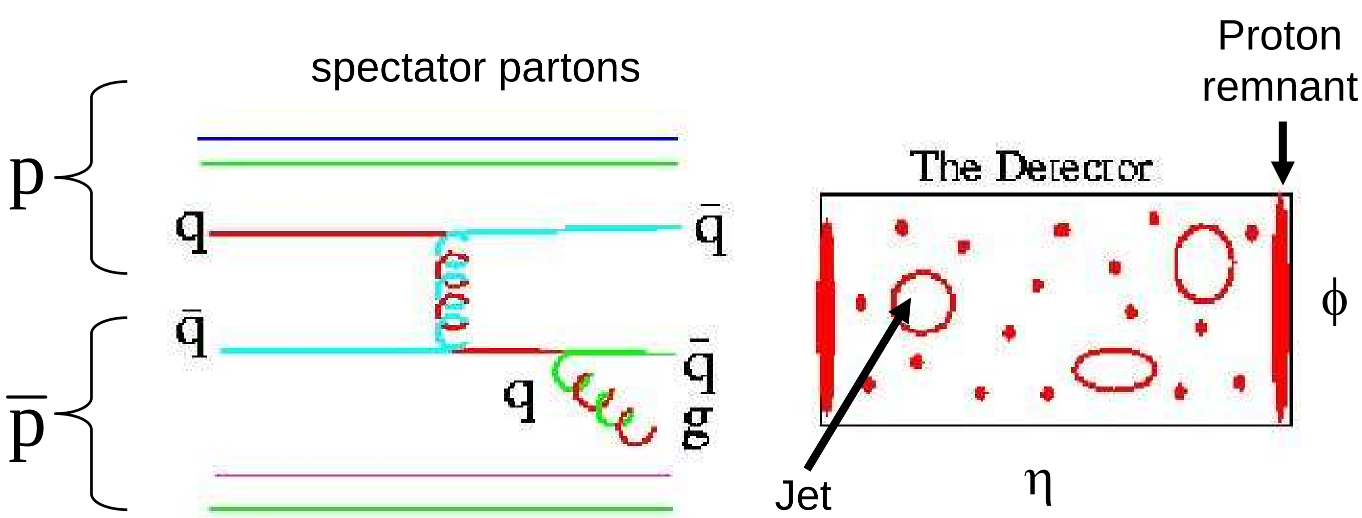

What is Diffraction?

- Diffraction in high energy hadron physics encompasses those phenomena in which no quantum numbers are exchanged between interacting particles
  - Surviving particles have same quantum numbers as incident particles
- Exchanging quanta of the vacuum is synonymous with Pomeron ($\mathbb{P}$) exchange
  - Named after Russian physicist I.Y. Pomeranchuk
  - Virtual particle which carries no net charge, isospin, baryon number or color
  - Couples through internal structure
- Can occur in hadron-hadron and lepton-hadron collisions
- Signatures of diffraction include rapidity gaps (regions of the detector with no particles above threshold) and tagging the intact final particle(s) with a forward detector
- Diffractive and elastic events account for ~40% of the total cross section at ~2 TeV

Examples of Soft Diffraction

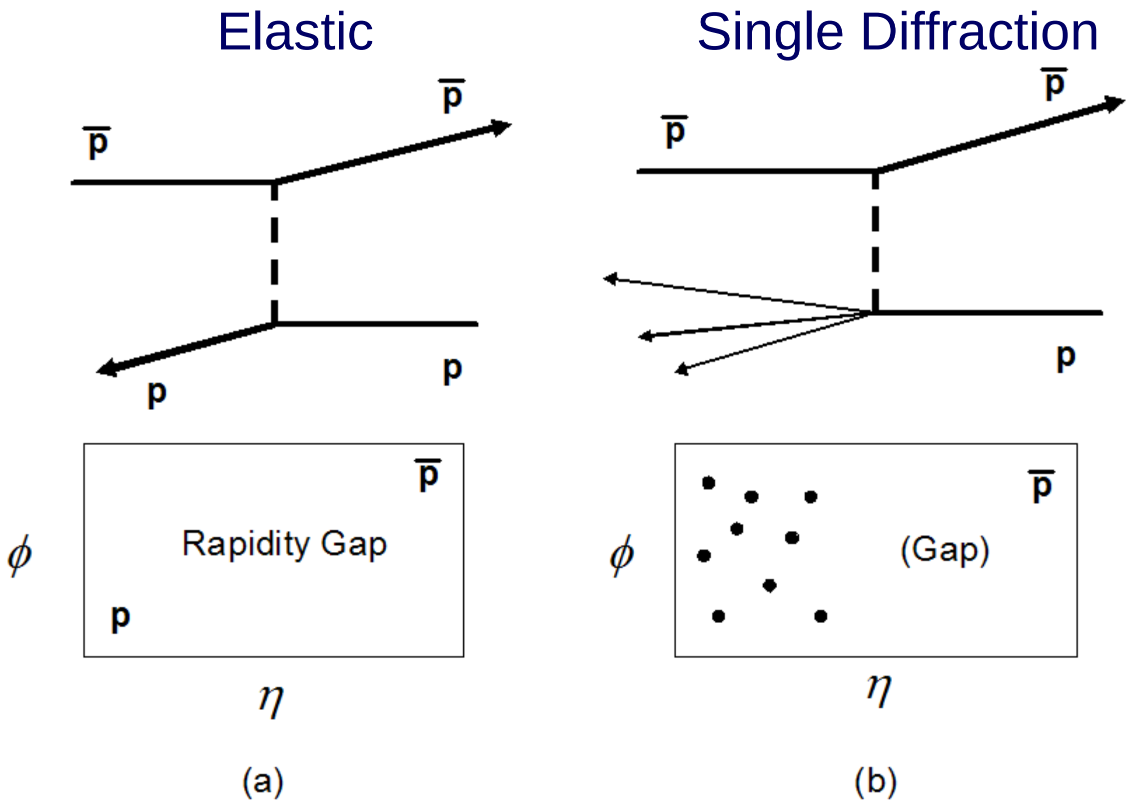

- Modeled by Regge Theory
  - Analysis of poles in the complex angular momentum plane give rise to trajectories that describe particle exchange
    - P.D.B. Collins, An Introduction to Regge Theory and High Energy Physics, Cambridge Univ. Press, Cambridge 1977
- Non-perturbative QCD
- Elastic cross section has same form as light diffracted from an absorbing disk, hence the name diffraction

Examples of Hard Diffraction

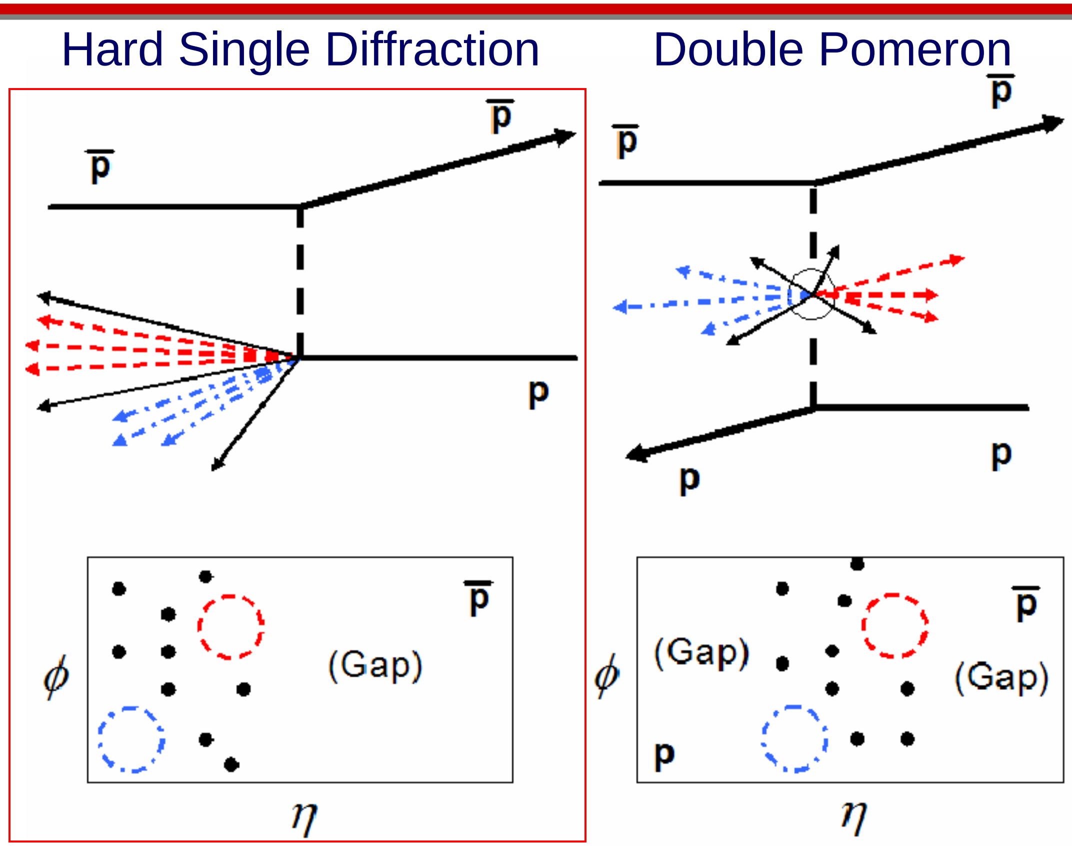

- Described by Different Models
  - Ingelman-Schlein (q/g partonic structure of Pomeron, trying to marry Regge to QCD)
    - G. Ingelman and P. Schlein, Phys. Lett. B **152**, 256 (1985)
  - BFKL based (gluon ladder structure of Pomeron)
    - L.N. Lipatov, Sov. J. Nucl. Phys. **23**, 338 (1976); E.A. Kuraev, L.N. Lipatov and V.S. Fadin, Sov. Phys. JETP **44**, 443 (1976); Sov. Phys. JETP **45**, 199 (1977); Y.Y. Balitsky and L.N. Lipatov, Sov. J. Nucl. Phys. **28**, 822 (1978)
  - Soft Color Interactions (non-perturbative effects of standard QCD, no Pomeron)
    - R. Enberg, G. Ingelman, and N. Timneanu, Phys. Rev. D **64**, 114015 (2001).

Diffractive Particle Kinematics

- The total center of mass energy is $\sqrt{s}$
  - This is 1.96 TeV for the Tevatron Run II
- The standard four-momentum transfer $|t|$ is defined as
  - $|t| = (p^{\mu}_{f} - p^{\mu}_{i})^2 \sim p^2\theta^2$ (for small angles)
- The momentum fraction (ξ) taken by the Pomeron is defined as
  - $\xi = 1 - x_p = 1 - p_f / p_i$
- Diffraction dominates for $\xi < 0.05$
  - For elastic, $\xi = 0$
- Diffractive mass (M_x) available is
  - $M_x = \text{sqrt}(\xi \cdot s)$
    - At $\sqrt{s} = 1.96$ TeV, $M_x = 440$ GeV for $\xi = 0.05$

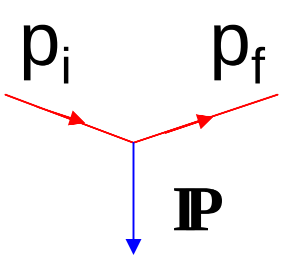

Calorimeter and Luminosity

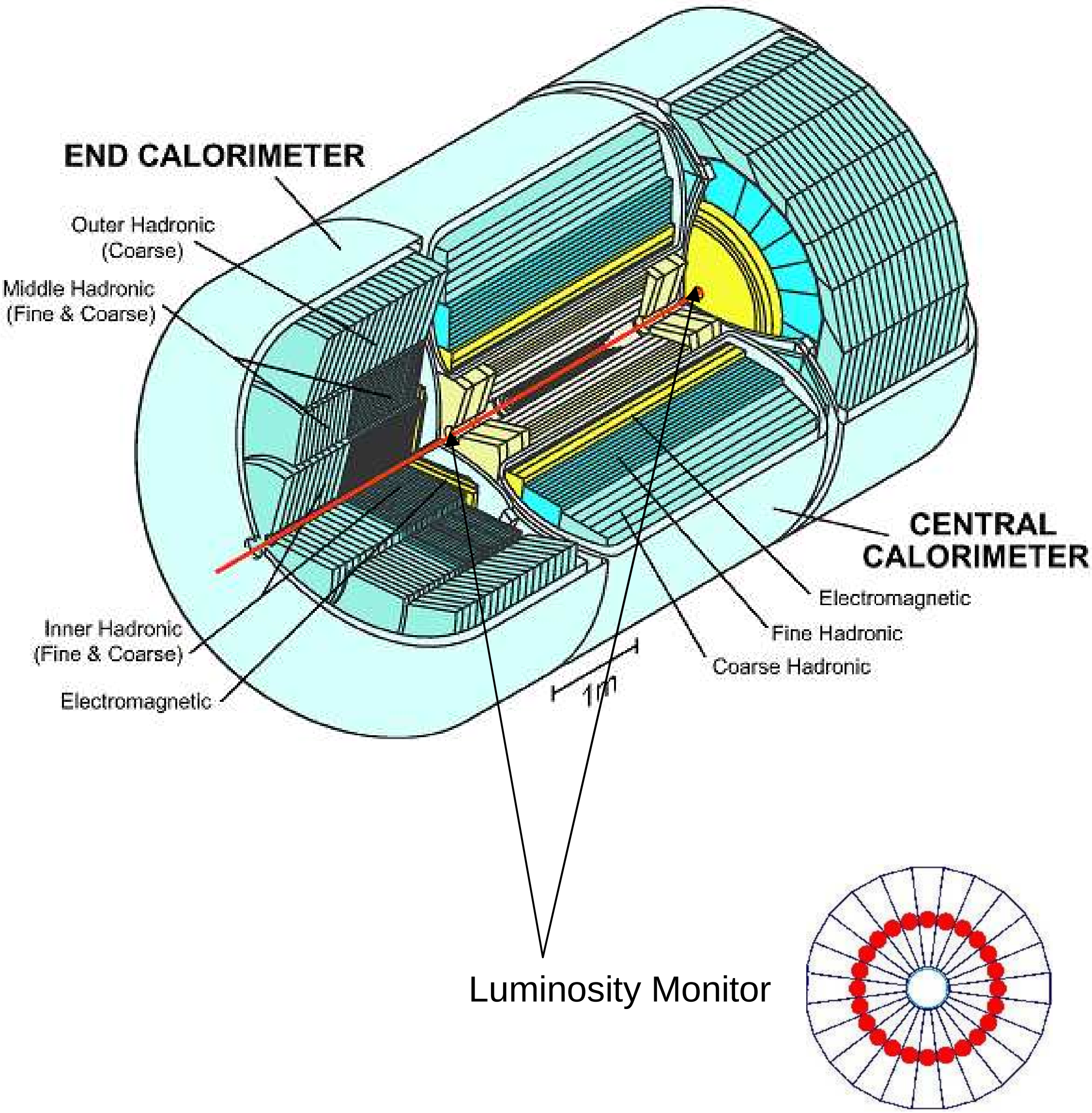

- Compensating calorimeter using depleted uranium and liquid argon
- Electromagnetic (EM), Fine Hadronic (FH) and Coarse Hadronic (CH) layers
- Central Calorimeter
  - $|\eta_{det}| < 1.0$
- Intercryostat Region
  - $0.8 < |\eta_{det}| < 1.4$
- End Calorimeter
  - EM $1.3 < |\eta_{det}| < 4.1$
  - Had $0.7 < |\eta_{det}| < 5.3$

- Luminosity Monitor
  - $|z| \approx 140$ cm
  - $2.7 < |\eta_{det}| < 4.4$

Forward Proton Detector Layout

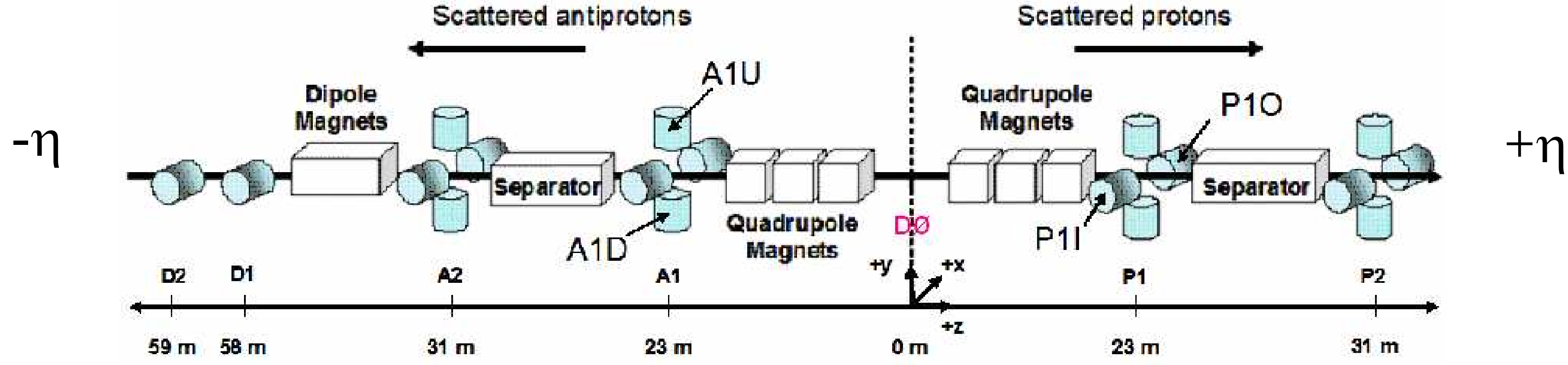

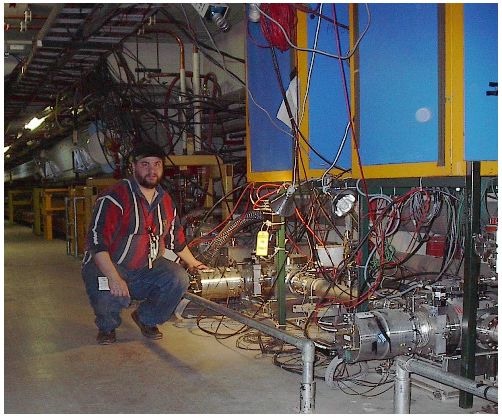

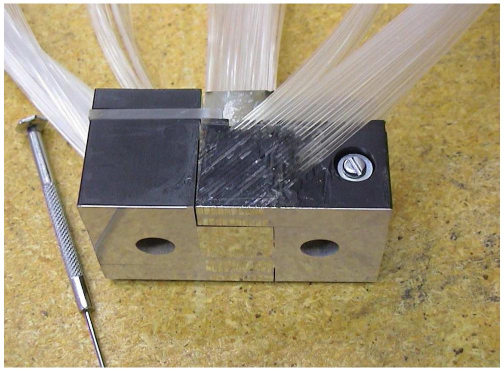

- **9 momentum spectrometers** composed of **18 Roman Pots**
- **Scintillating fiber detectors** can be brought close (~6 mm) to the beam to **track scattered protons and anti-protons**
- Reconstructed track is used to calculate momentum fraction and scattering angle
  - Much better resolution than available with gaps alone
- Cover a t region ($0 < t < 4.5$ GeV^2) never before explored at Tevatron energies
- Allows combination of tracks with high-p_T scattering in the central detector

FPD Detector Setup

- 6 layers per detector in 3 planes and a trigger scintillator (for timing and L1 trigger)
- u and v at ±45 degrees with respect to bottom of detector, x at 90 degrees
- u and v layers have 20 fibers, x layers have 16 fibers
- Layers in a plane offset by ~2/3 fiber
- Each channel filled with four fibers
- 2 detectors in a spectrometer

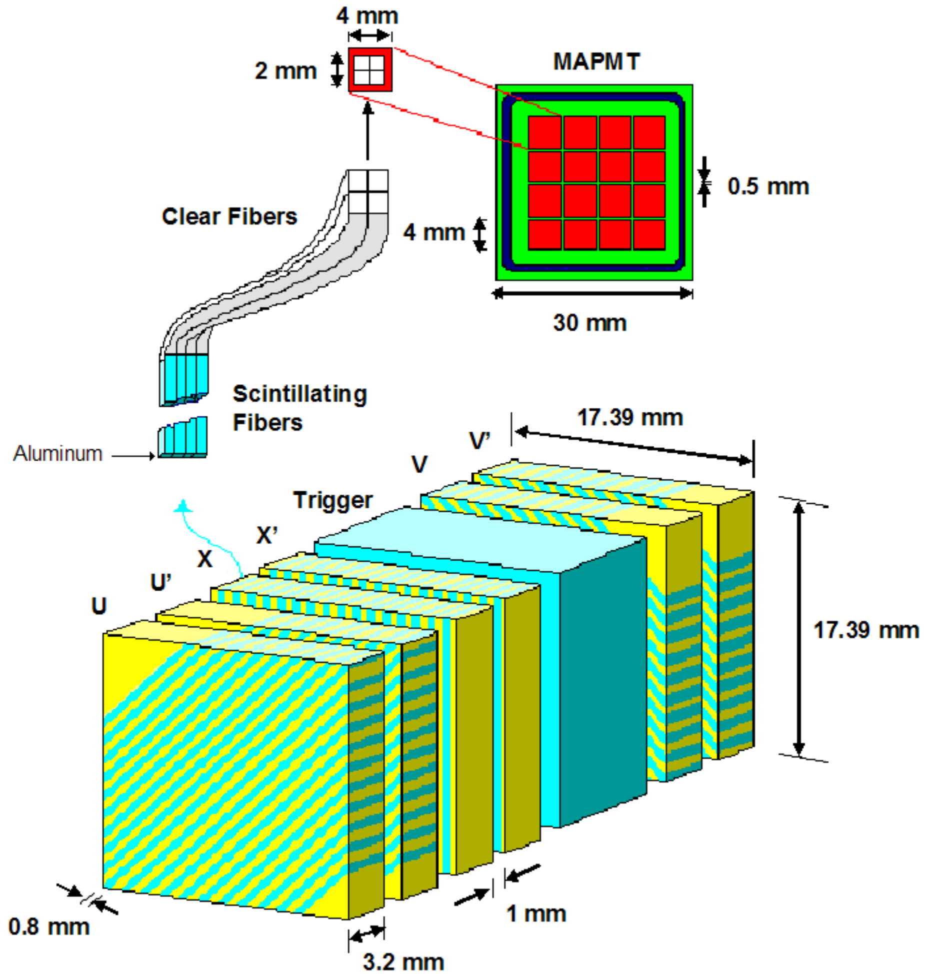

FPD Detector Assembly

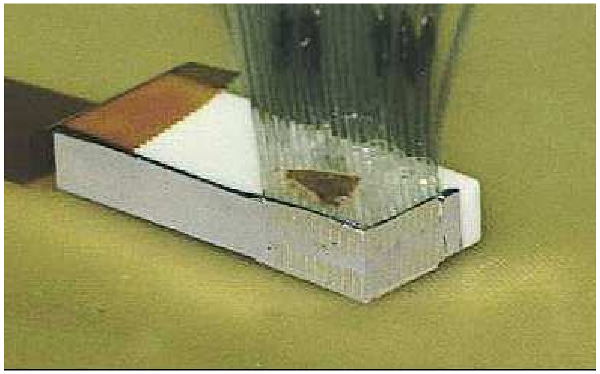

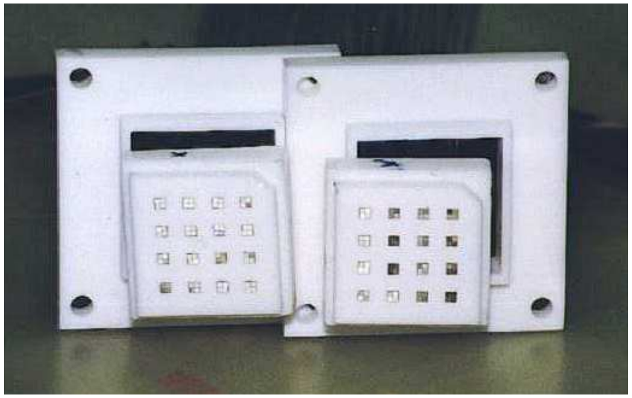

- Scintillating fibers are aligned in channels of the detector frame and secured with optical epoxy
- Trigger scintillator is secured in x frame
- Clear fibers are aligned in plastic support (cookie) which provides the interface between the detector and the readout MultiAnode Photomultiplier Tubes (MAPMTs)
- Detector planes are assembled and all edges are polished. Ends of scintillating fibers are aluminized
- Detector is mounted in an aluminum cartridge base which allows the detector to be placed in the castle located in the tunnel and aligns elements with the readout electronics.

Dipole Antiproton Prototrack

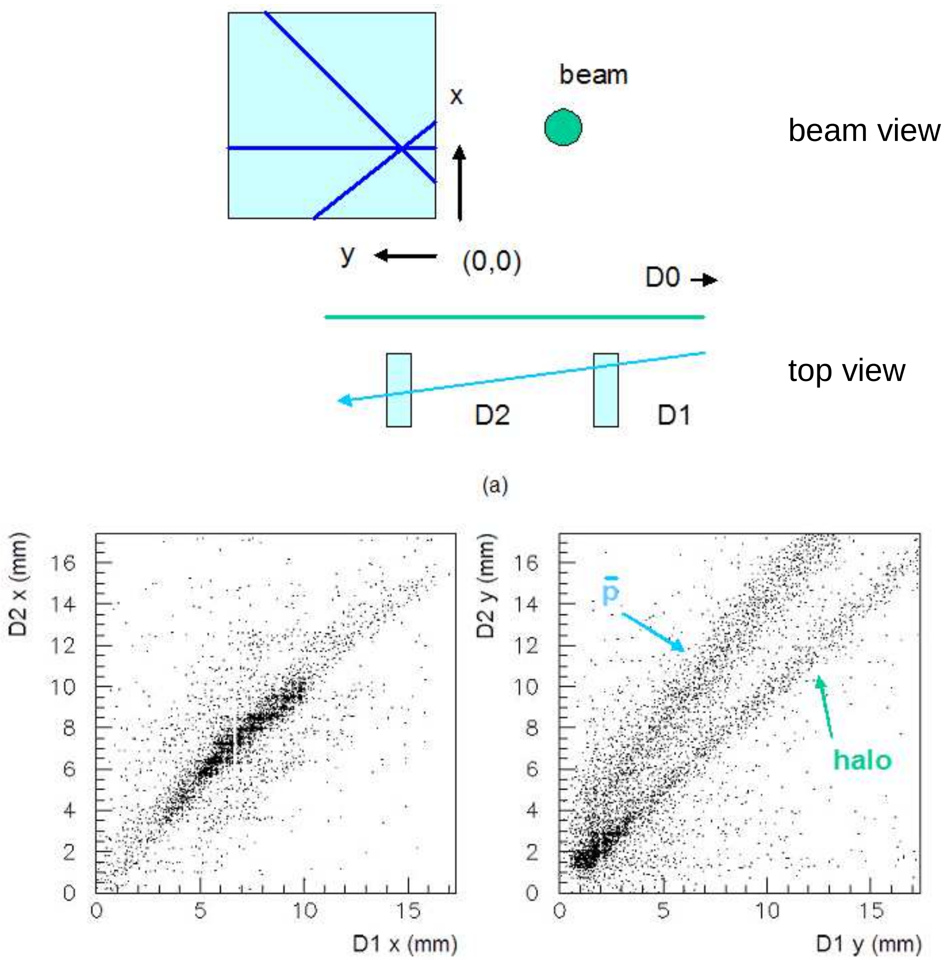

- In events with hits in each detector of the spectrometer, the hits tend to fall in correlation bands
- Due to the location of the dipole spectrometer, particles from the next incoming bunch can be passing through the detector at the same time as outgoing particles.
- Diffracted antiprotons have lost a fraction of their momentum, and therefore are bent more by the dipole magnets leading to a noticeable angle between hits in the detector
- Halo particles have beam momentum and therefore do not exhibit this angle
- Particles in the upper y_d correlation band are prototracks

Theoretical Reconstruction Resolution and Acceptance

- Monte Carlo propagates particles of known ξ_0 and t_0 to the detectors, where the hits are then reconstructed to arrive at a theoretical resolution

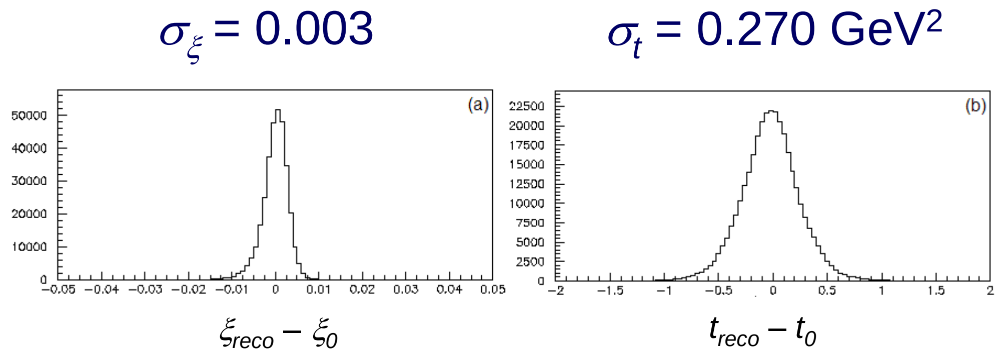

- Spectrometer has an acceptance in ξ and t .
    - shown for flat-|t| dependence and pots at 14σ positions

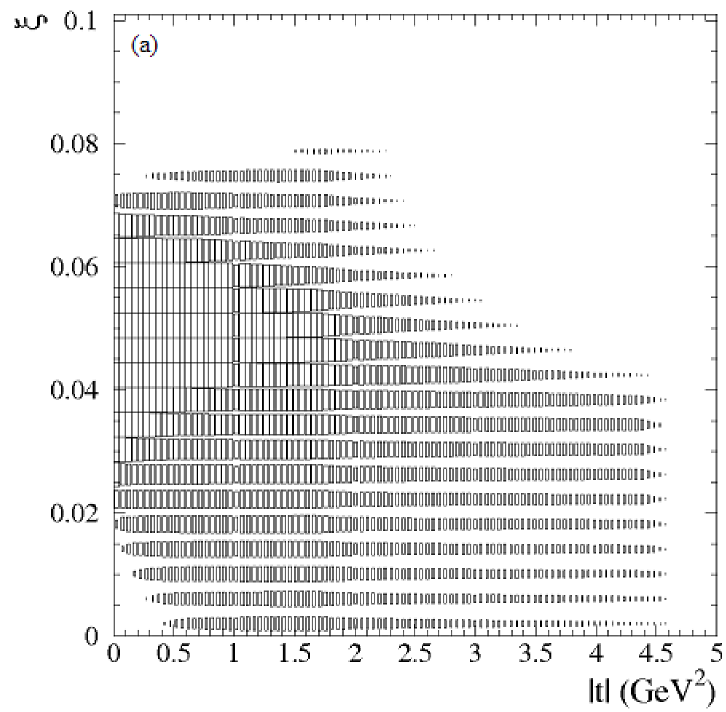

- Accurate reconstruction relies on knowing the relative alignment of the detectors relative to each other in the spectrometer as well as relative to the beam

Hit Correlations

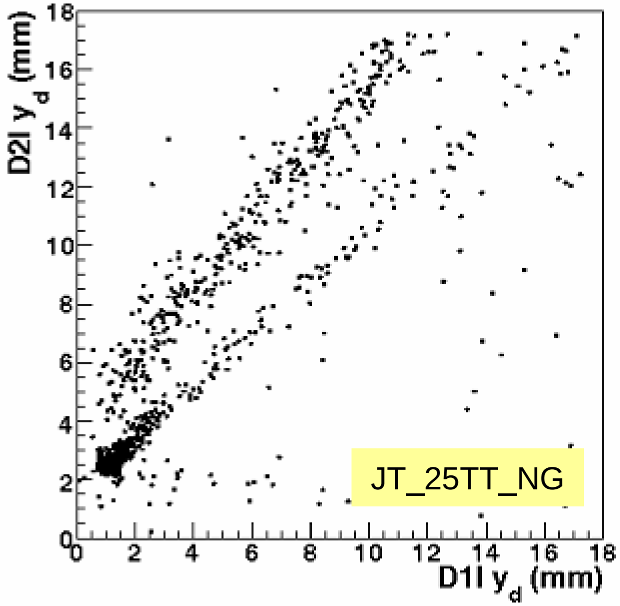

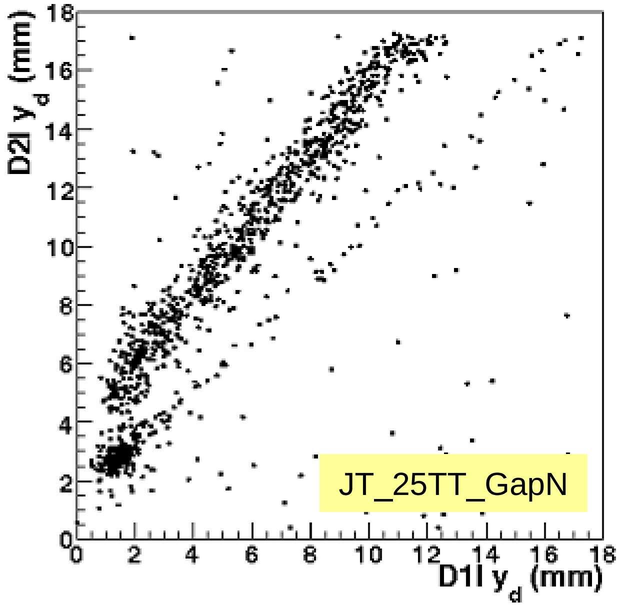

- Correlation bands are present
- In-time (prototrack) band is strongest for JT_25TT_GapN as expected

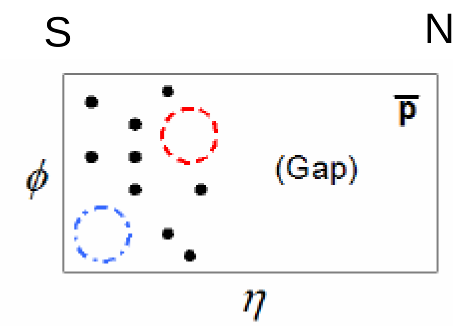

Effect of tags on Missing Et

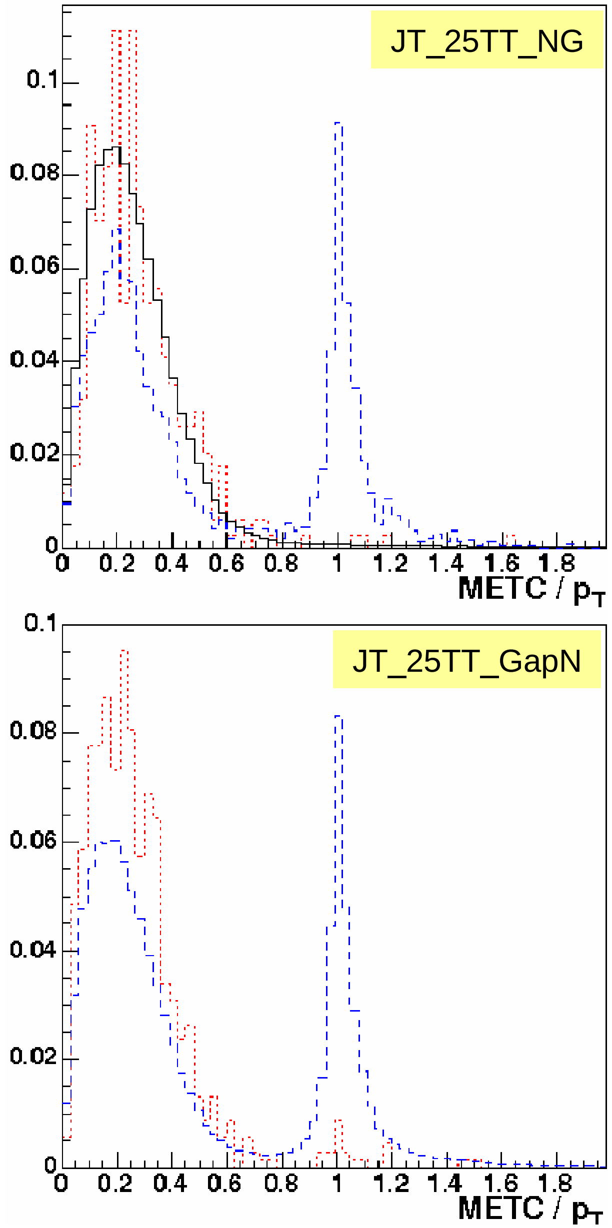

- All following plots have the same format:
  - Black plot shows distribution for events with no tags or gaps
  - Blue shows distribution for gaps
    - Alone, could indicate instrumental effect leading to one jet that is unbalanced resulting in mEt
  - Red shows distribution for tags
- See the expected noise peak at METC/p_T = 1 in the gap sample
- The inclusion of a tag suppresses the fake peak, indicating that it is correlated with real activity in the central detector

η distributions of jets

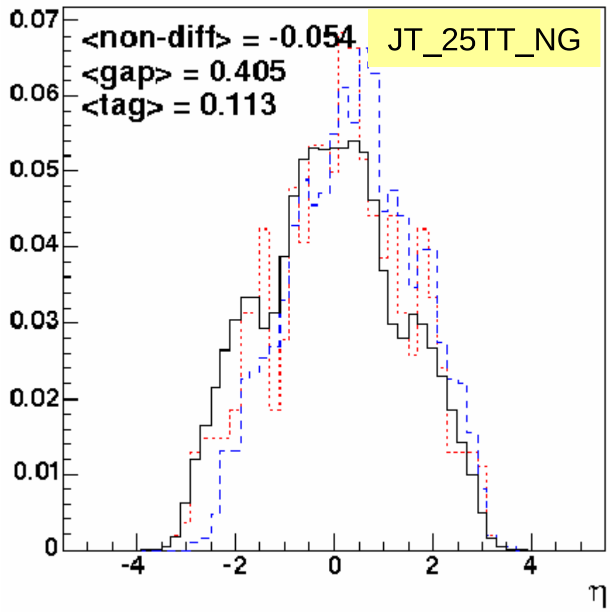

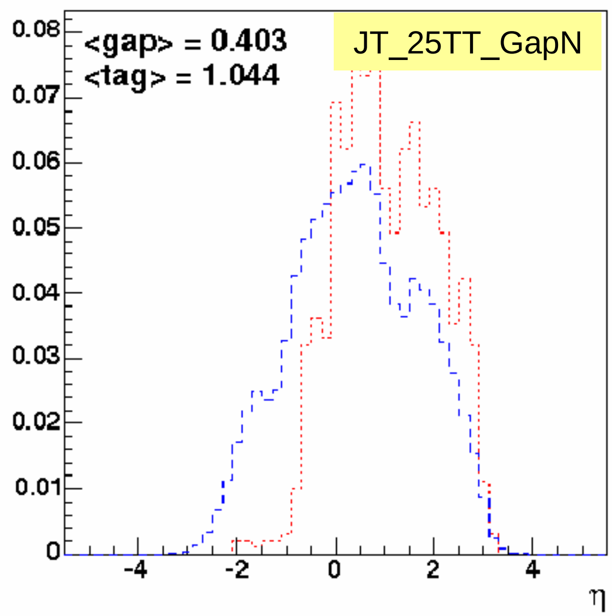

- Jet η is expected to be boosted away from the side of the detector with a gap/tag
  - There is a suppression of activity on the side of the detector with the gap
  - Kinematics require that as the mass of the event increases, the momentum fraction of the parton in the proton increases, leading to a boosted system

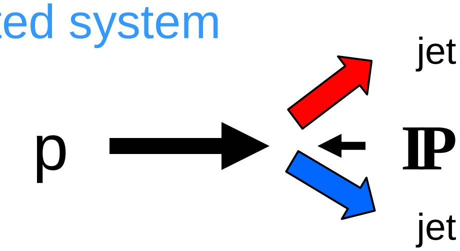

- Gap sample is shifted as expected
- For tagged events in the gap sample, the acceptance of the dipole spectrometer "fixes" the ξ, leading to the kinematic boost

Track Reconstruction

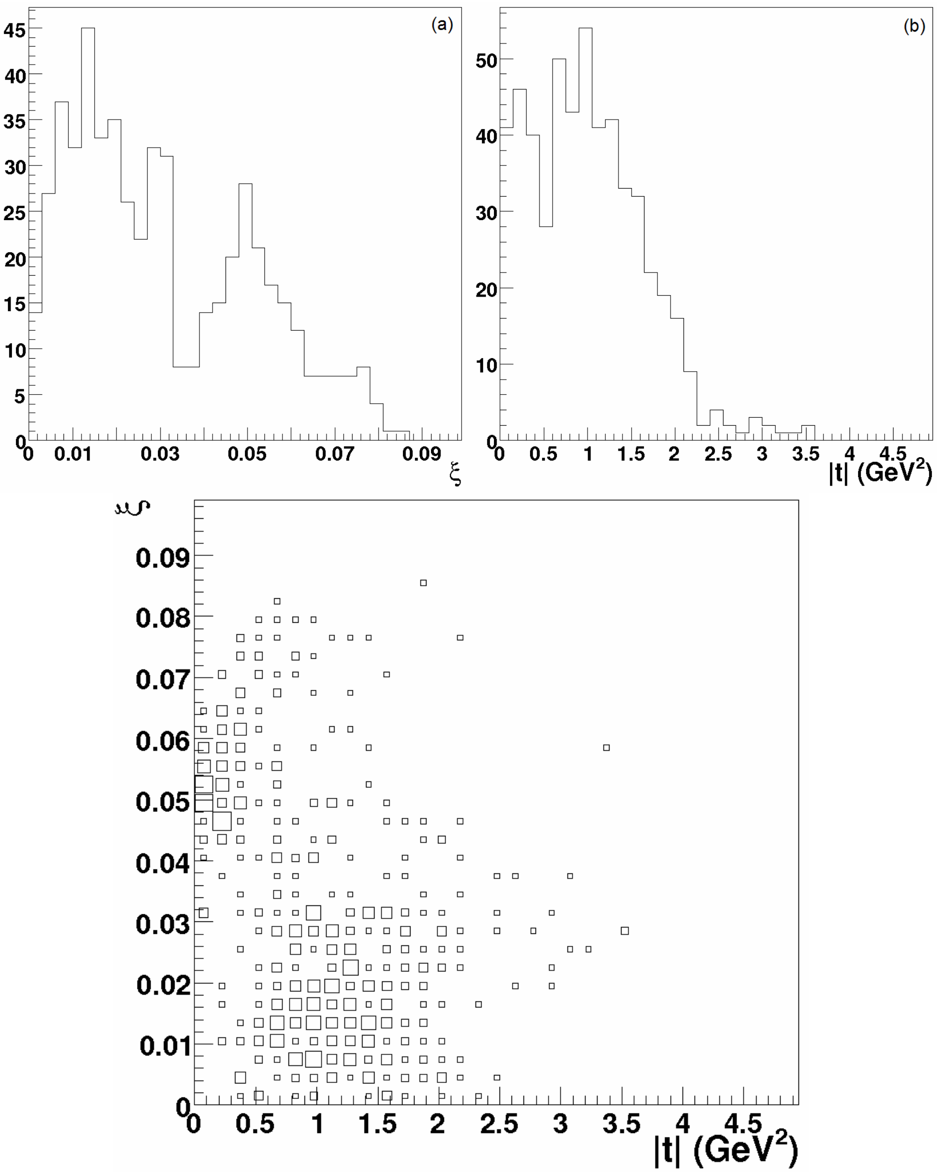

- Obtain ξ and *t* from the tracking algorithms
- Trigger selection gives two regions
  - Gaps are biased towards lower ξ
- Since most of the prototracks come from a gap trigger, the low-ξ is disproportionate to the cross section.
- ξ-*t* correlation follows expected behavior of acceptance:
  - High-ξ with low-*t*
  - Low-ξ to high-*t*

CMS Software Validation

Software Validation

- The Software Validation Suite (SVS) is a group of packages used to perform release-to-release validation of the software chain in the new CMSSW framework:
  - It includes generator, simulated hit, digitized hit, reconstructed hit,…, tower,…, track,…, jet, e,… level packages which create a set of histograms to be automatically compared against references at the time the suite is run (before each release).
- It is designed to run over pre-generated samples (particle gun, minbias, physics signal) that are processed through the full chain of standard software.
- It is being built by a cross-boundary group including generator, simulation, reconstruction developers and Detector-Physics group representatives who recommend plots of interest to detect changes/bugs between releases

CMS Detector

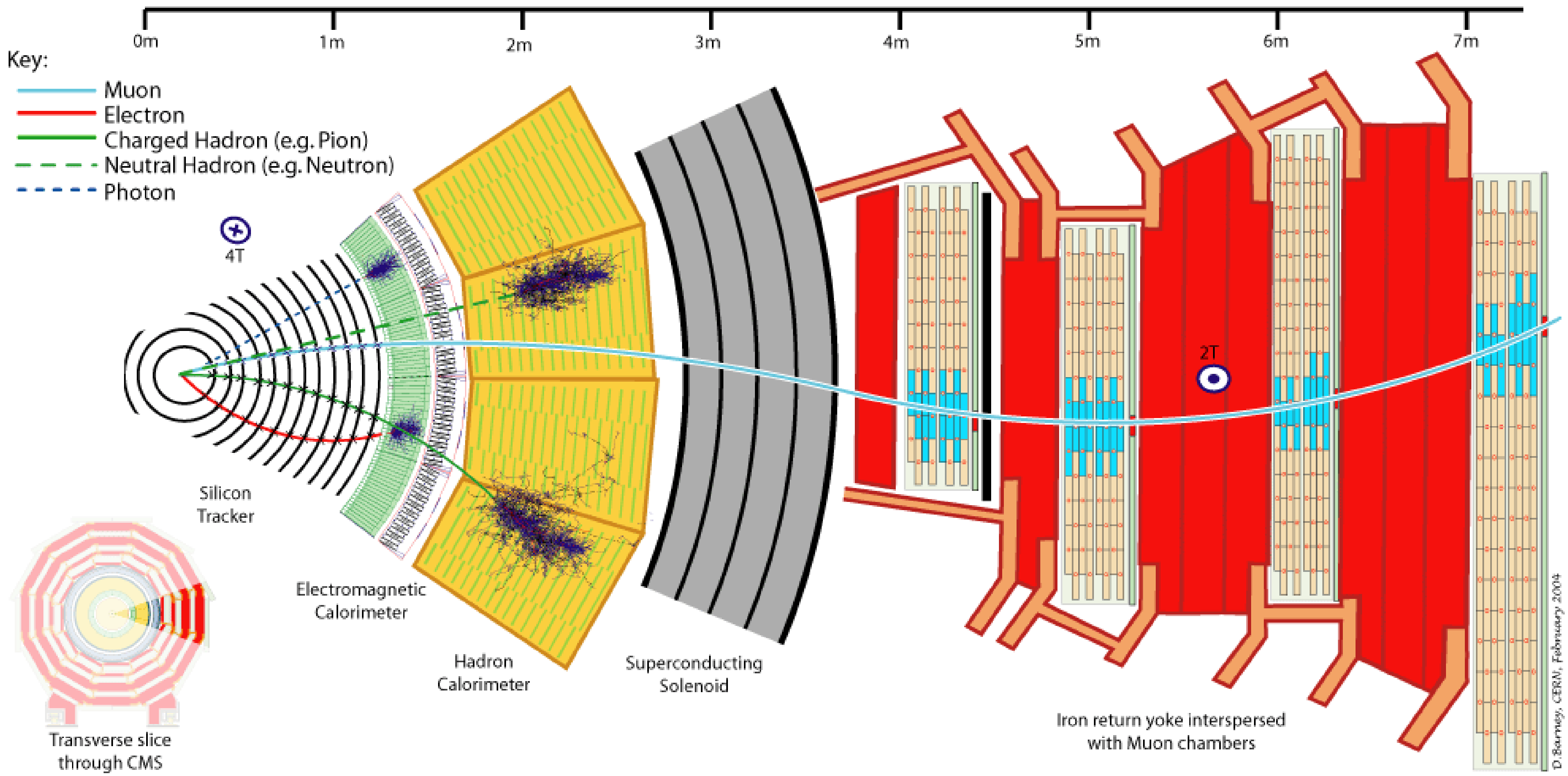

Design Philosophy

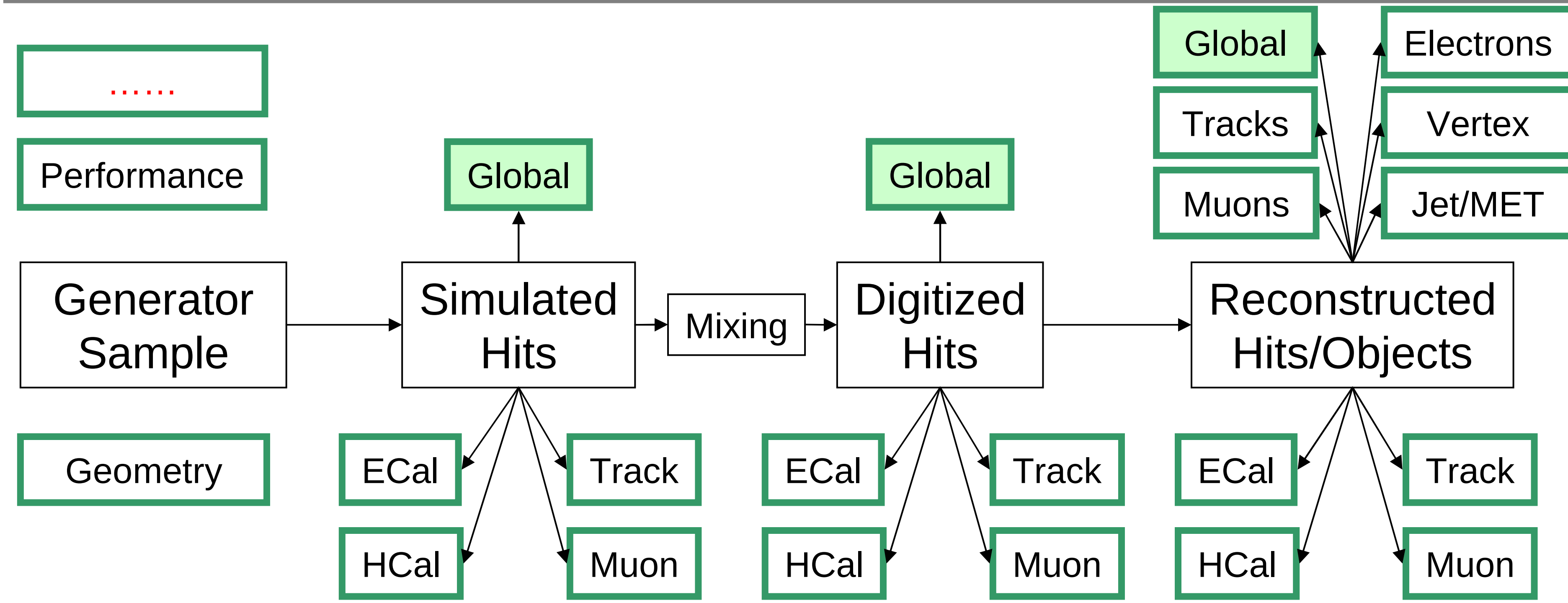

- Individual system packages look at the information in local coordinates with other subsystems turned off in the geometry
- Global packages look at all sub-detectors with full magnetic field in global coordinates
- Special packages look at different aspects like geometry of subsystems for material budget, performance, etc.
- Digi level and higher uses data quality management tools (DQM)

Work Flow for Simulation Validation

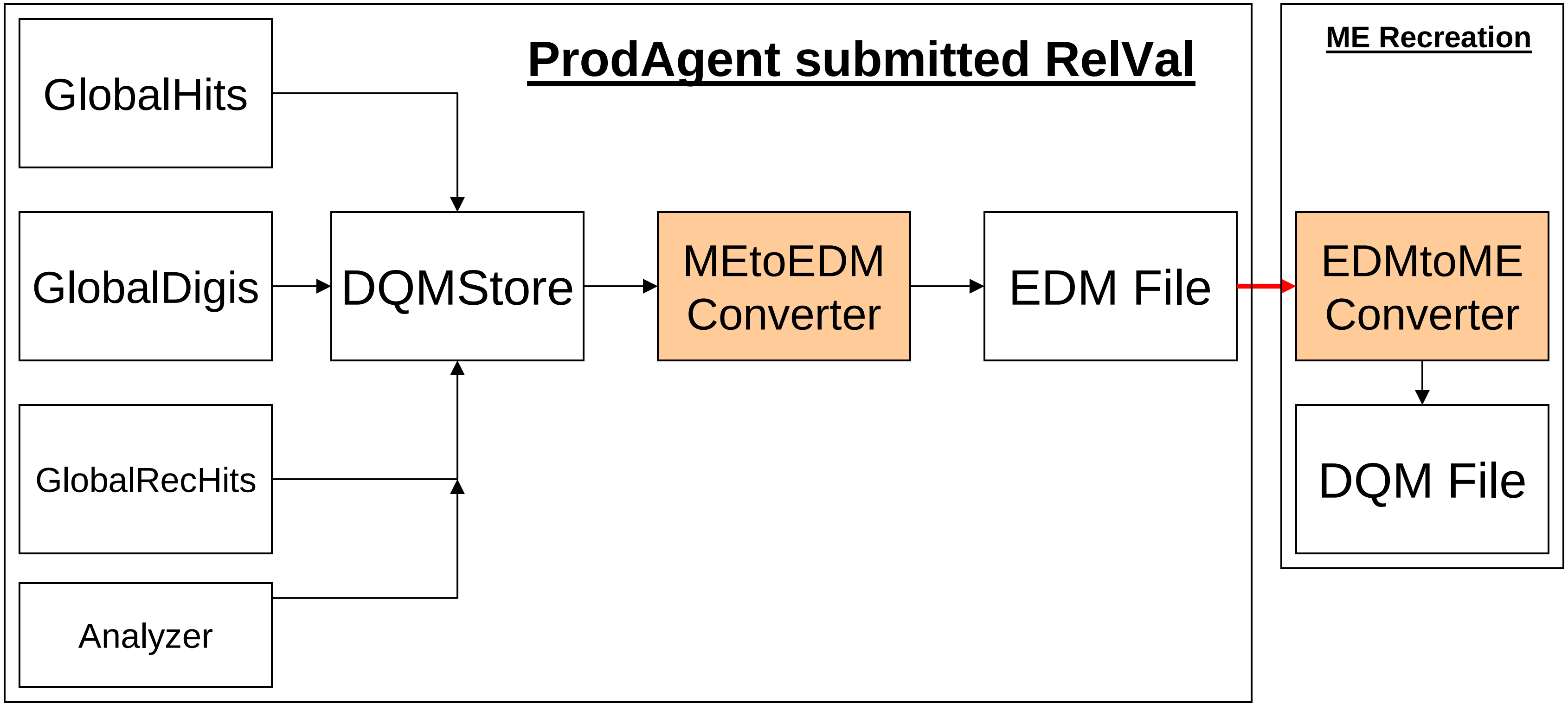

- Validation analyzers declare monitor elements (ME) via DQMStore in constructor
- MEtoEDMConverter accesses the DQMStore to find what monitor elements exist
  - extracts the necessary information from the ME to store in the data format that is stored in the Run tree of the EDM file.
- EDMtoMEConverter accesses the information in the Run tree and uses the modified clone method of the ME (to merge results) to reconstruct contents of original DQM root file
- This DQM file can then be compared against reference using standard DQM tools

DØ ZZ Observation

Diboson Physics at the Tevatron

- Measure production cross sections
- Probe gauge boson self-interactions
  - Consequence of non-Abelian nature of $SU(2)_L \otimes U(1)_Y$
  - One of the least tested areas of the SM
- Sensitive to new physics in trilinear gauge couplings (TGC)
  - Different combinations of couplings
  - Evidenced by increase in measured cross section relative to Standard Model
- Probe for new heavy resonances decaying into dibosons
- Backgrounds to numerous channels:
  - Higgs; SUSY; ttbar

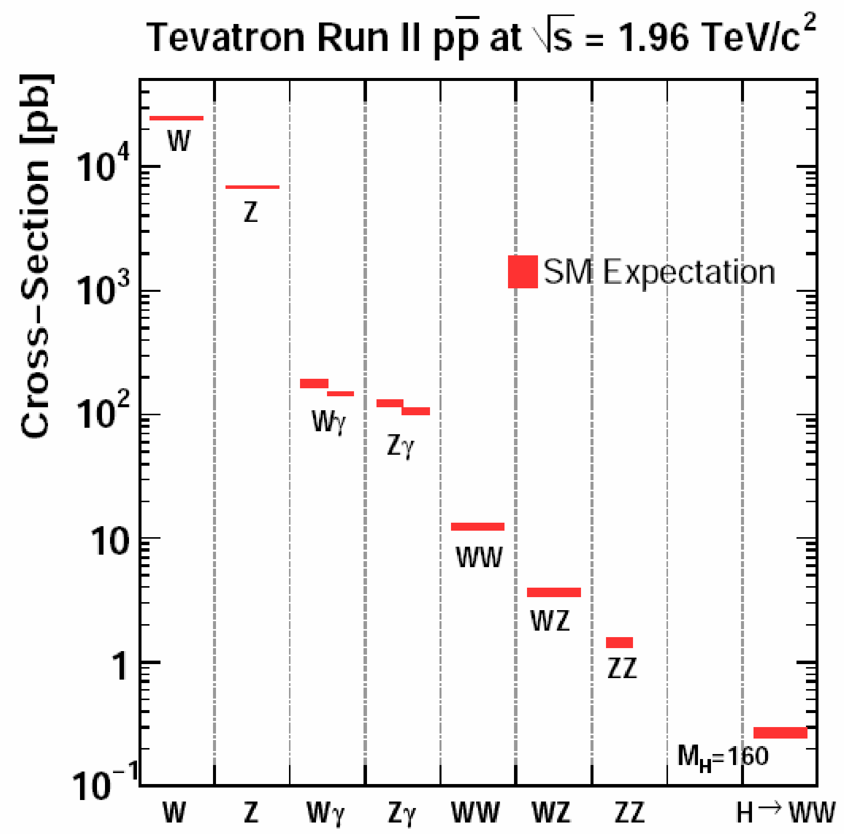

note: this is σ, not $\sigma \times$ BR

Previous DØ Diboson Results

Wγ
Preliminary cross section
Indication of radiation amplitude zero
PRD 71, 091108 (2005)
PRL 100, 241805 (2008)

Zγ
Cross section measured
Limits on ZZγ and Zγγ couplings
PLB 653, 378 (2007)

WW
Cross section measured
PRL 94, 151801 (2005)

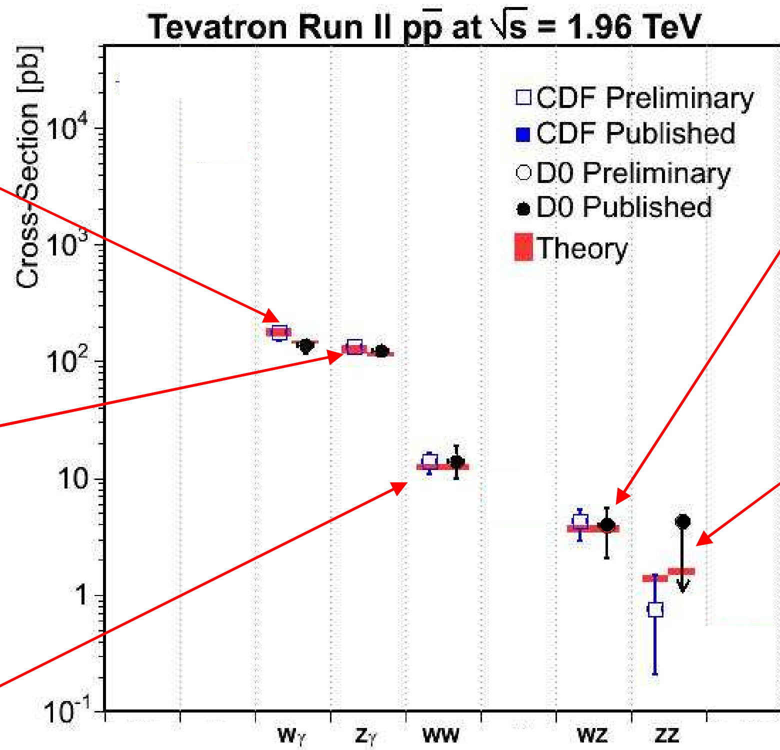

WZ
First evidence
Limits on WWZ couplings
PRD 76, 111104(R) (2007)

ZZ
Cross section limit
Limits on ZZZ and ZZγ*
couplings
PRL 100, 131801 (2008)

ZZ Production

- Very small production cross section
  - $\sigma^{NLO}(ZZ) = 1.4 \pm 0.1$ pb

    [J.M. Campbell and R.K. Ellis
    PRD 60, 113006 (1999)]
    - sqrt(s): 2.0→1.96 GeV
    - $\alpha = 1 / 128.89$
    - $\sin^2(\theta_w) = 0.2312$
    - PDFs to CTEQ6.6M

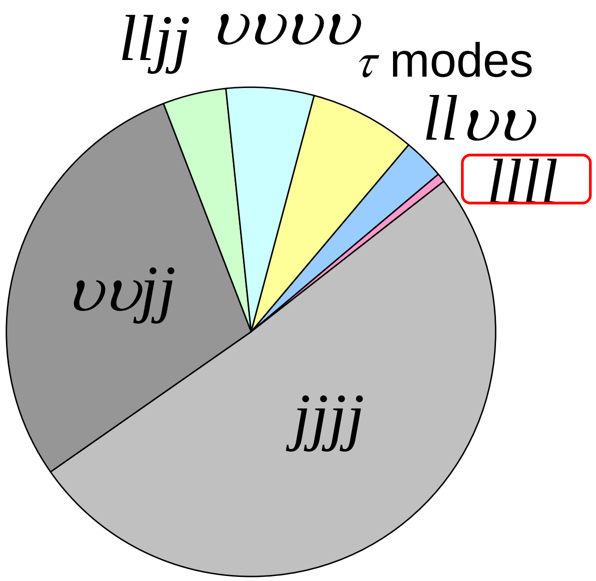

- decay mode studied:
  - $ZZ \rightarrow llll$, with l = e or μ
    - Very clean: low background contamination from Z/γ+jets and ttbar processes
    - Very smaller BR = $(2 \times 0.033)^2 = 0.0044$
    - Look directly for four lepton signature

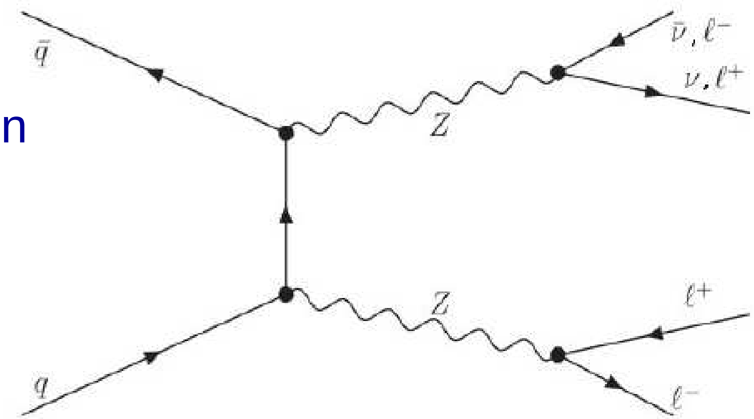

Data

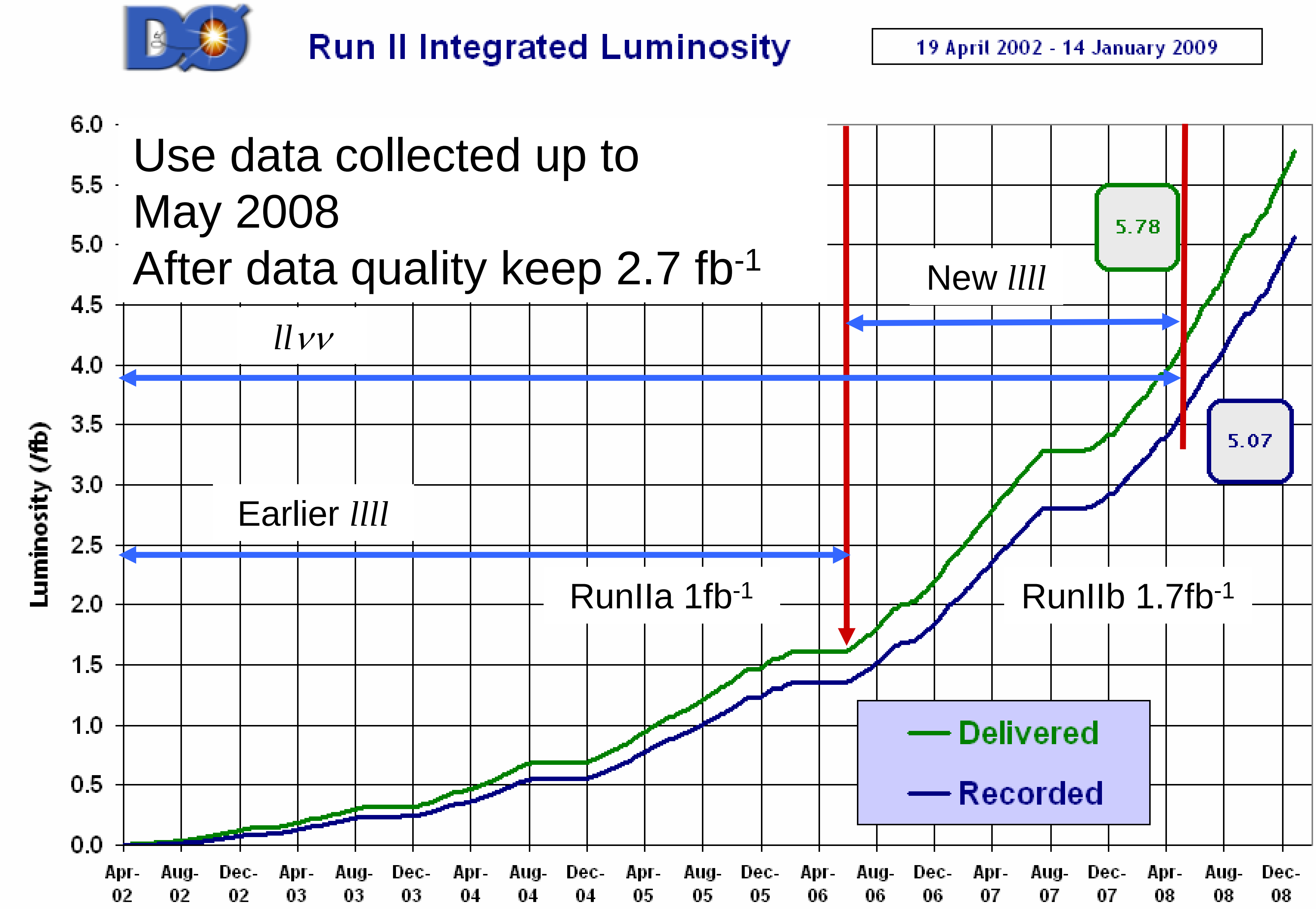

Run II Integrated Luminosity
19 April 2002 - 14 January 2009
Use data collected up to May 2008
After data quality keep 2.7 fb-1
New llll
llνν
Earlier llll
RunIIa 1fb-1
RunIIb 1.7fb-1
5.78
5.07
Delivered
Recorded
Luminosity (/fb)
6.0
5.5
5.0
4.5
4.0
3.5
3.0
2.5
2.0
1.5
1.0
0.5
0.0
Apr-02
Aug-02
Dec-02
Apr-03
Aug-03
Dec-03
Apr-04
Aug-04
Dec-04
Apr-05
Aug-05
Dec-05
Apr-06
Aug-06
Dec-06
Apr-07
Aug-07
Dec-07
Apr-08
Aug-08
Dec-08

The DØ Detector

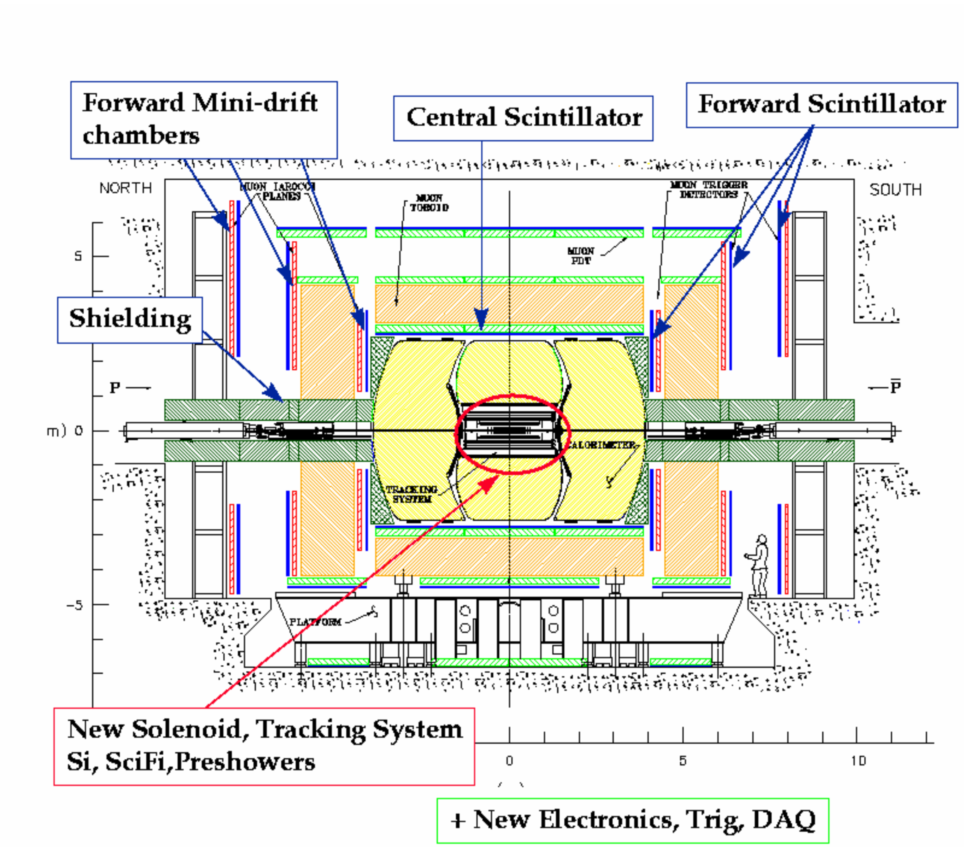

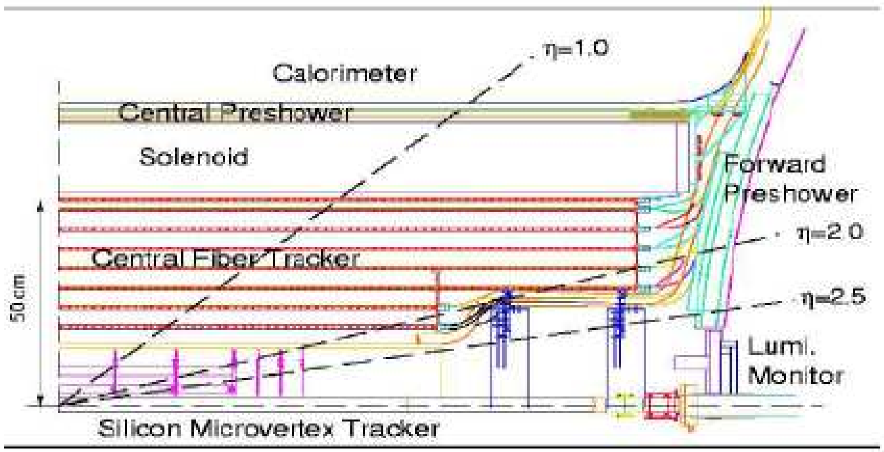

- Silicon micro-strip vertex detector
- Scintillating fiber tracker
- 2 T solenoid magnet
- Uranium Liquid Argon calorimeter
- 1.8 T toroid magnet
- Wire tracking / scintillation counter muon detector
- Pseudorapidity coverage:
  - Electrons: $|\eta| < 3.2$
  - Muons: $|\eta| < 2.0$

Electron Selection

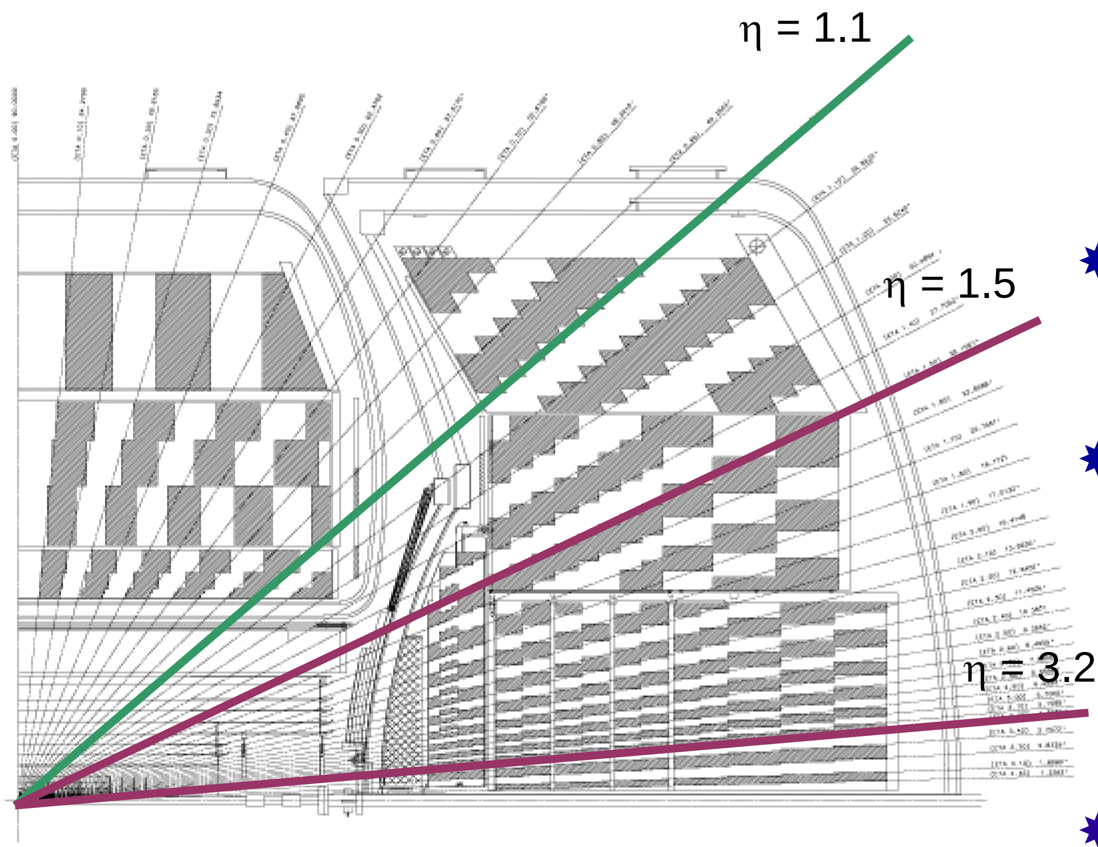

- Must be reconstructed either in the central $|\eta| < 1.1$ or forward $1.5 < |\eta| < 3.2$ EM calorimeter
- Must be isolated from other energy clusters
- Central electrons must be matched to a track and satisfy a cut on multi-variate parameter of energy and shower distribution
- Forward electrons not required to have track, but must satisfy more stringent shape requirements

Muon Selection

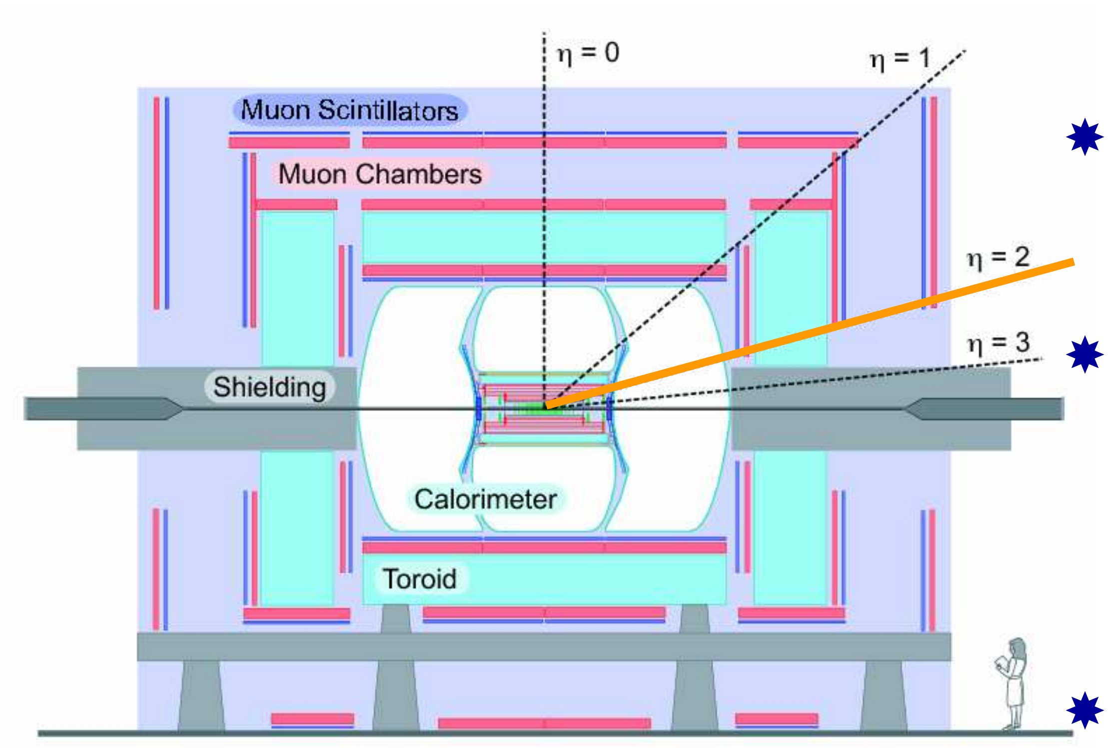

- Must be matched to a central track
- Must satisfy timing requirements in the muon detector
- Track must satisfy a distance of closest approach cut
  - < 0.02 cm w/ SMT hits
  - < 0.2 cm w/o SMT hits
- Must satisfy calorimeter isolation requirements if not enough hits in the muon system

Mass cut

- As it is impossible to differentiate between Z and γ^* quantum mechanical states experimentally, we must set a mass cut a priori at which we decide to call the observed particle a Z. This is based on Z/γ^* Z/γ^* PYTHIA Monte Carlo:

- $M(Z_1) > 70$ GeV, $M(Z_2) > 50$ GeV

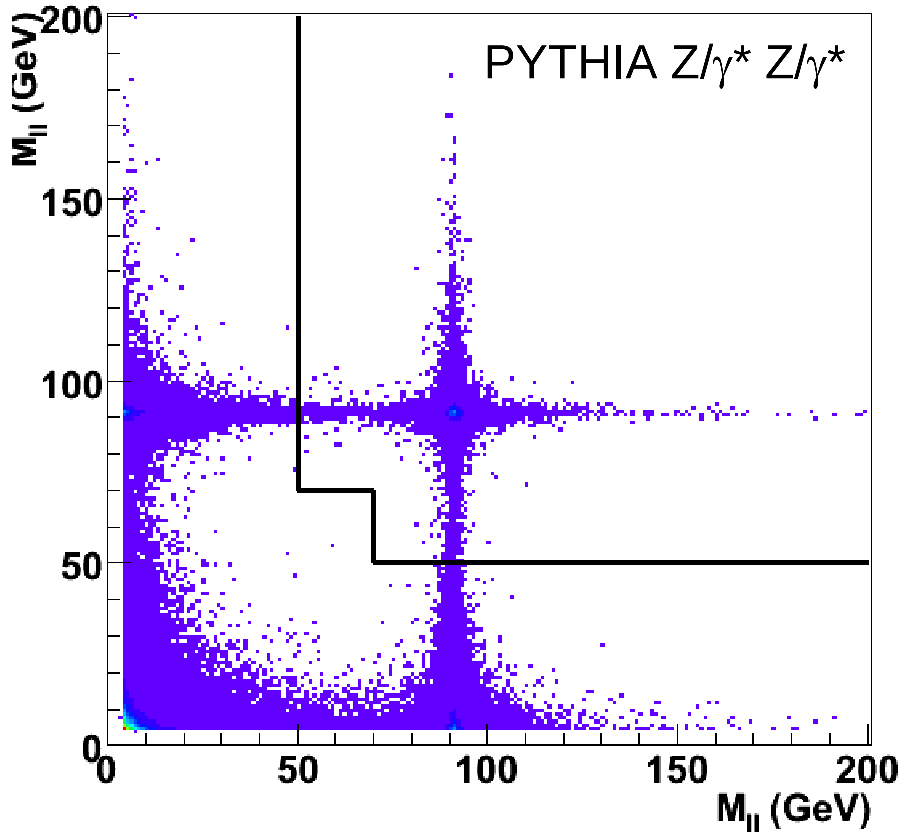

Event Selection

- Common Requirements
  - Require passage of OR of single and di-lepton triggers
  - Require 4 well reconstructed leptons
    - $p_{T1} > 30$ GeV, $p_{T2} > 25$ GeV, $p_{T3} > 15$ GeV, $p_{T4} > 15$ GeV
  - $M_1(ll) > 70$ GeV, $M_2(ll) > 50$ GeV
- 4e
  - Break into subchannels of 2, 3 or 4 central electrons
    - QCD background expected to decrease based on number of track matched electrons
- 4μ
  - Require at least three calorimeter isolated muons to reduce ttbar background
  - Cosine of angle between all pairs < 0.96 to reduce misreconstruction
  - Require tracks to originate from primary vertex
- $2e2\mu$
  - Require passage of common triggers OR electron-muon triggers
  - Require two well reconstructed electrons and muons
    - $p_{T1} > 25$ GeV, $p_{T2} > 15$ GeV in both cases
  - Break into subchannels of 0, 1 or 2 central electrons
  - Require isolation (for at least one muon), angle and track requirement as muons
  - $\Delta R > 0.2$ between electrons and muons to remove inclusive $Z \rightarrow \mu\mu$ events where muons radiate a photon

Expectation

- Use PYTHIA Monte Carlo passed through GEANT simulation
  - Normalize to luminosity using mass cut on MC truth mass of the Z bosons
- Apply appropriate cut flow
- For signal expectation, also include small contribution from case where Z decays to τ pair which then decays to satisfy cut flow requirement
- For ttbar background, use a sample of ttbar→2b+2l+2ν

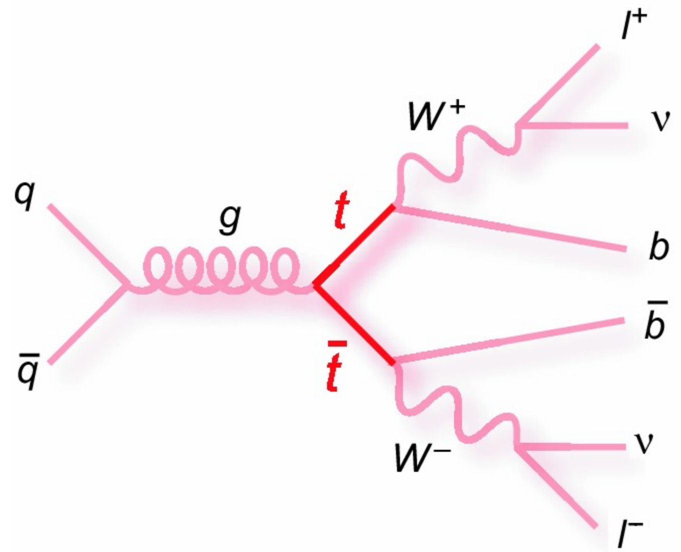

- End with acceptance x efficiency which is used to extract the expected yield

Lepton Misidentification

- Calculate lepton misidentification rate of jets using tag and probe method from data
  - Require two jets, one of which must pass tight requirements (tag) and the other (probe) is in the opposite direction
  - Look for good leptons in the event that are near the probe jet

Require some energy in EM calorimeter, energy in the hadronic calorimeter not caused by “hot” cells in detector

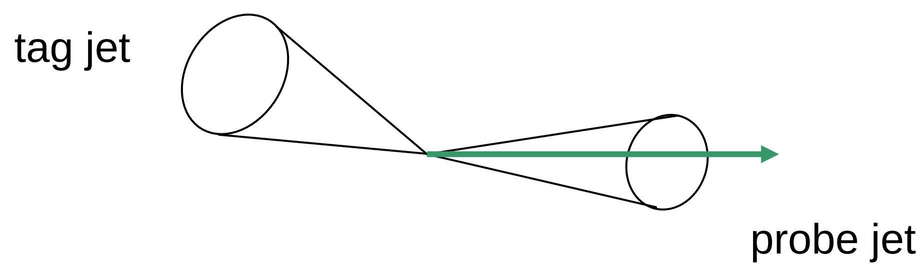

  - Ratio of events where probe jet is associated to a lepton to all probe jets is the misidentification rate
    - For electrons, this is parameterized in terms of η and p_T and is on the order of 4×10^{-4} for central jets and 5×10^{-3} for forward jets
    - For muons, this is parameterized in terms of tag jet p_T and probe jet η for different muon pT and isolation. For jets of p_T = 15 (100) GeV that aren’t isolated is on the order of 10^{-4} (10^{-2}) and if isolated 10^{-5} (10^{-4})

QCD Background

- Misidentification rate is then applied to data requiring jets in the final state
- For 4e look at 3e+jet, for 2e2μ look at 2μ+e+jet and 2e+2jets final states to account for contributions from Z+γ+jets where the γ has been converted to an electron, plus Z/W/WZ/WW+jet contributions
  - This method double counts the contribution from Z+jets, so is corrected by finding the contribution from 2e+2jet and 2μ+2jet final states. This correction is O(20%).
- For the 4μ channel, just use 2μ+2jet final state, but no mass cut is applied since the kinematics between muons and jets is different

Systematics

- Systematics are dominated by the following:
  - Signal:
    - 4% (2.5%) uncertainty on lepton identification and reconstruction efficiencies for 4e,4μ (2e2μ)
    - 6.1% uncertainty in luminosity
  - ttbar:
    - 10% from uncertainty in cross section and variation in cross-section and acceptance from uncertainty in top mass
  - QCD:
    - 30% due to uncertainty in misidentification rates estimated by varying selection criteria in control samples

Results

Subchannel	$4e_{2C}$	$4e_{3C}$	$4e_{4C}$	4μ	$2\mu 2e_{0C}$	$2\mu 2e_{1C}$	$2\mu 2e_{2C}$
Luminosity (fb^{-1})	1.75 ± 0.11	1.75 ± 0.11	1.75 ± 0.11	1.68 ± 0.10	1.68 ± 0.10	1.68 ± 0.10	1.68 ± 0.10
Signal	0.084 ± 0.008	0.173 ± 0.015	0.140 ± 0.012	0.534 ± 0.043	$0.058^{+0.007}_{-0.006}$	0.352 ± 0.040	$0.553^{+0.045}_{-0.044}$
$Z(\gamma)$+jets	$0.030^{+0.009}_{-0.008}$	$0.018^{+0.008}_{-0.007}$	$0.002^{+0.002}_{-0.001}$	0.0003 ± 0.0001	$0.03^{+0.02}_{-0.01}$	0.05 ± 0.01	$0.008^{+0.004}_{-0.003}$
$t\bar{t}$	–	–	–	–	$0.0012^{+0.0016}_{-0.0009}$	0.005 ± 0.002	$0.0007^{+0.0009}_{-0.0005}$
Observed events	0	0	2	1	0	0	0

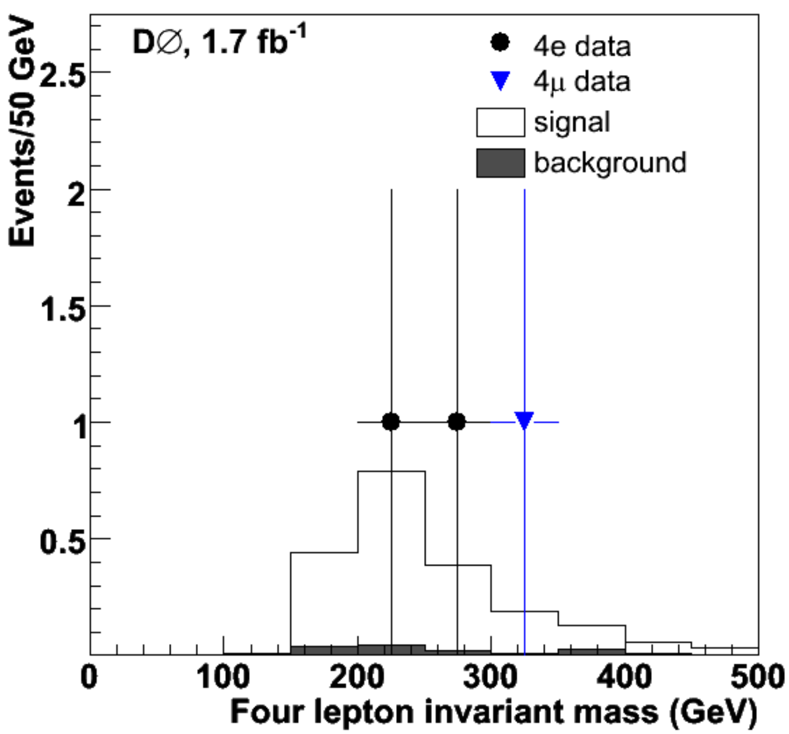

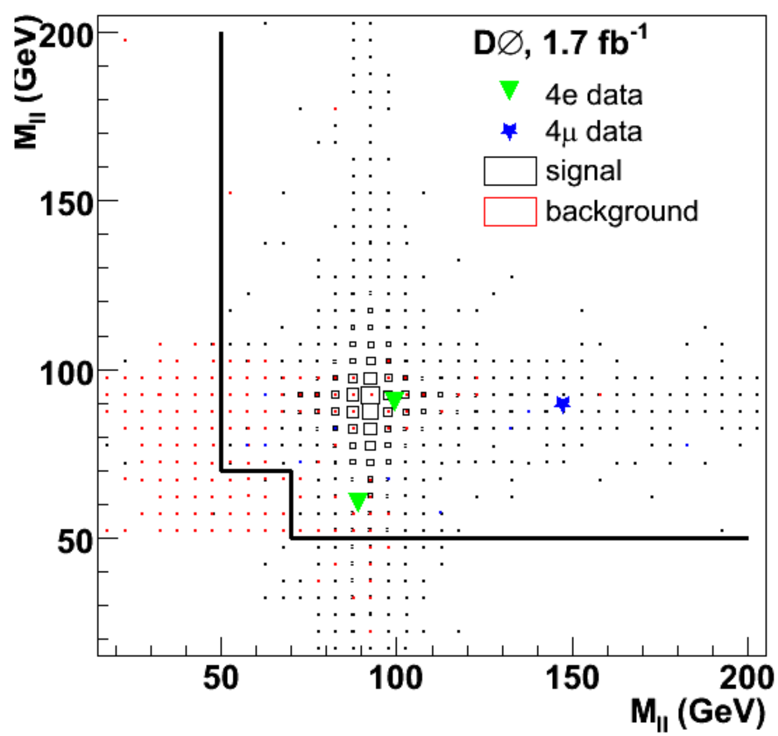

Candidate 1

		e_1^+	e_2^+	e_3^-	e_4^-
4e candidate 1	p_T (GeV)	107	59	52	16
	η	0.66	0.25	-0.64	-0.85
	ϕ	4.10	1.08	0.46	2.62
	$M_{\ell\ell}$ (GeV)	$e_1^+ e_4^-$ 89 ± 3		$e_2^+ e_3^-$ 61 ± 2	

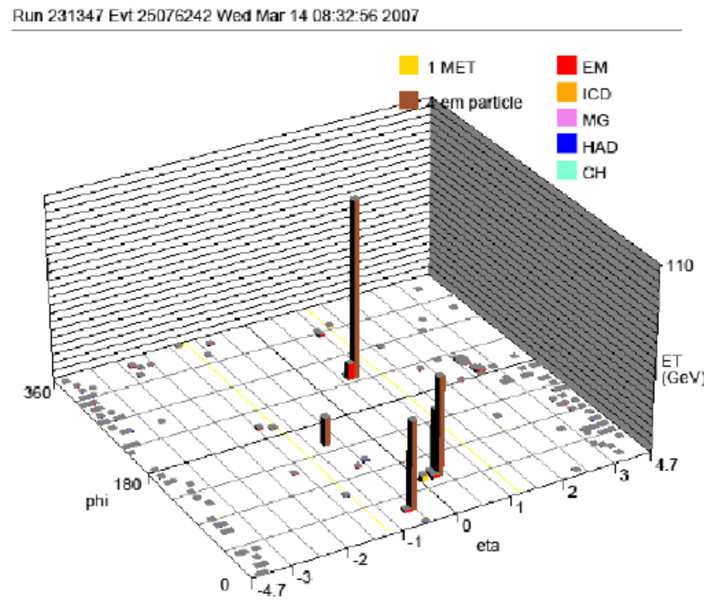

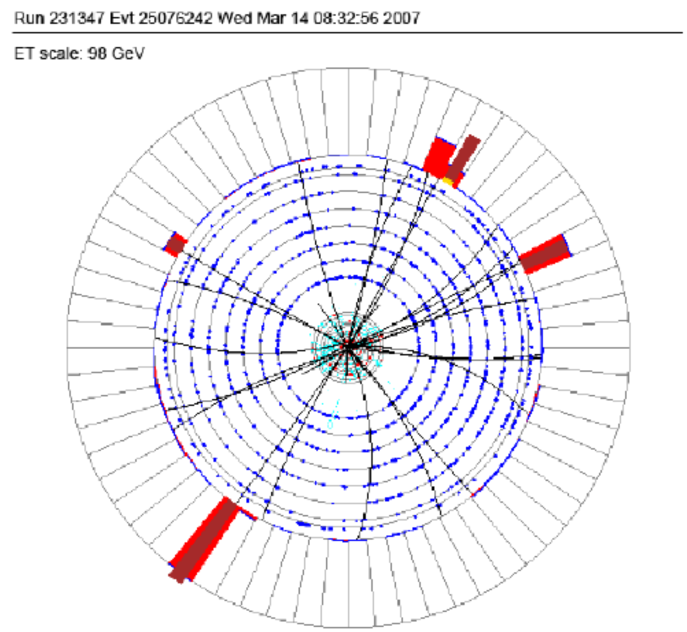

Candidate 2

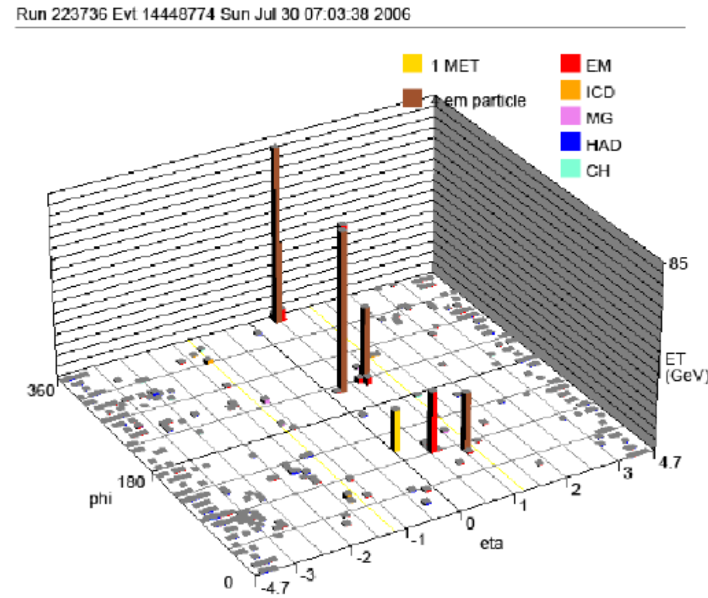

		e_1^+	e_2^+	e_3^-	e_4^-
$4e$ candidate 2	p_T (GeV)	83	75	35	26
	η	0.64	0.40	0.85	1.17
	ϕ	6.16	3.80	3.83	1.40
		$e_1^+ e_3^-$		$e_2^+ e_4^-$	
	$M_{\ell\ell}$ (GeV)	99 ± 3		90 ± 4	

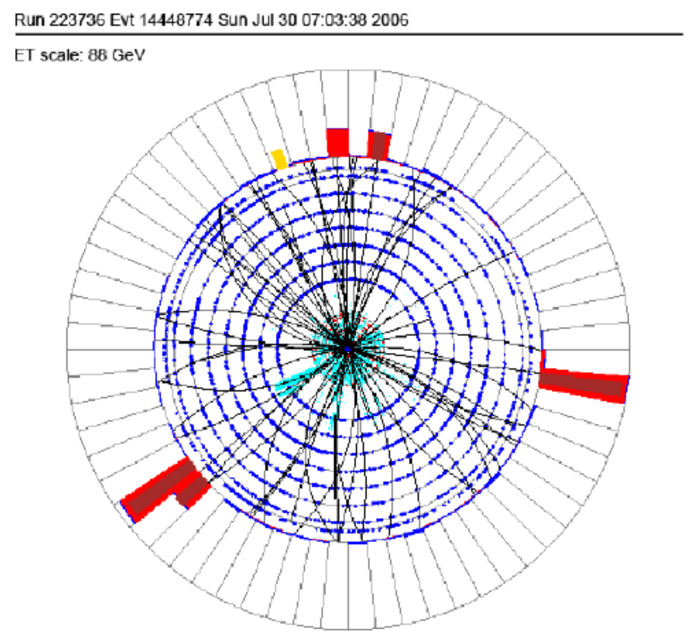

Candidate 3

		μ_1^+	μ_2^-	μ_3^-	μ_4^+
4μ candidate	p_T (GeV)	115	77	42	24
	η	0.04	-1.01	0.77	-1.93
	ϕ	1.69	4.26	5.29	0.36
	$M_{\ell\ell}$ (GeV)	$\mu_1^+\mu_3^-$ 148^{+32}_{-18}		$\mu_2^-\mu_4^+$ 90^{+12}_{-8}	

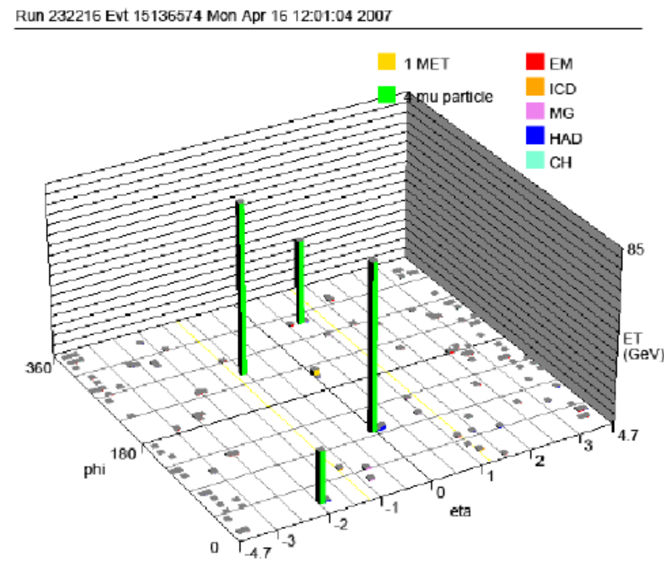

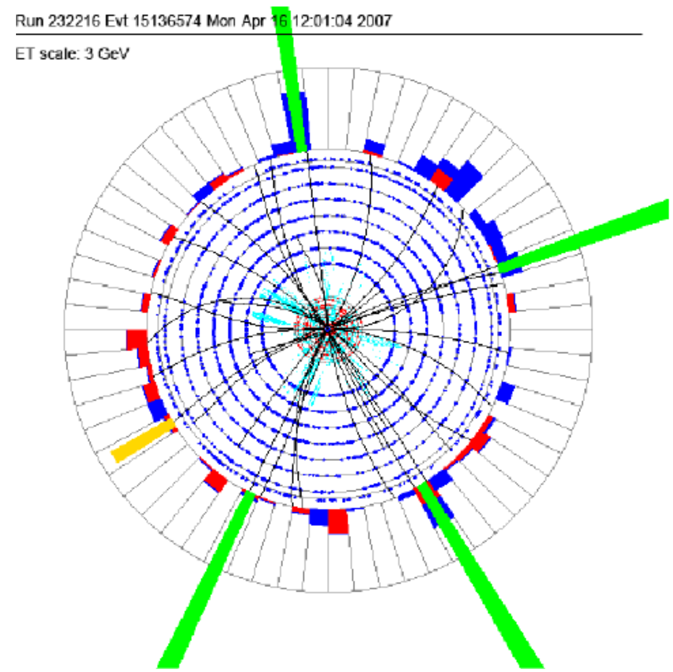

Significance

- Performed using a semi-frequentist approach
  - Assume data is drawn randomly from a Poisson parent distribution
- Input is the information in channels (binned)
  - s is expected signal, b is expected background, d is data
  - Generate pseudo-experiments via random Poisson with mean value from expected b and s+b
  - Systematic uncertainties treated using a Bayesian model
    - Treated as Gaussian-distributed, randomly sampled for each pseudo-experiment
    - Nominal background prediction varied according to smeared values of systematics, changing the mean of the random Poisson with each pseudo-experiment
- Use a negative log-likelihood ratio (LLR) test statistic:

$$LLR(\vec{s},\vec{b},\vec{d}) = \sum_{i=0}^{N_{bins}} s_i - d_i \ln(1+\frac{s_i}{b_i})$$

Significance Cont'd

- Input is the yields (number of events) in each of the seven sub-channels
- In 5 x 10^9 pseudo-experiments, find 213 trials with an LLR value more signal like than that observed
  - Equates to a p-value of 4.3 x 10^{-8}
  - 5.3σ (3.7σ expected)

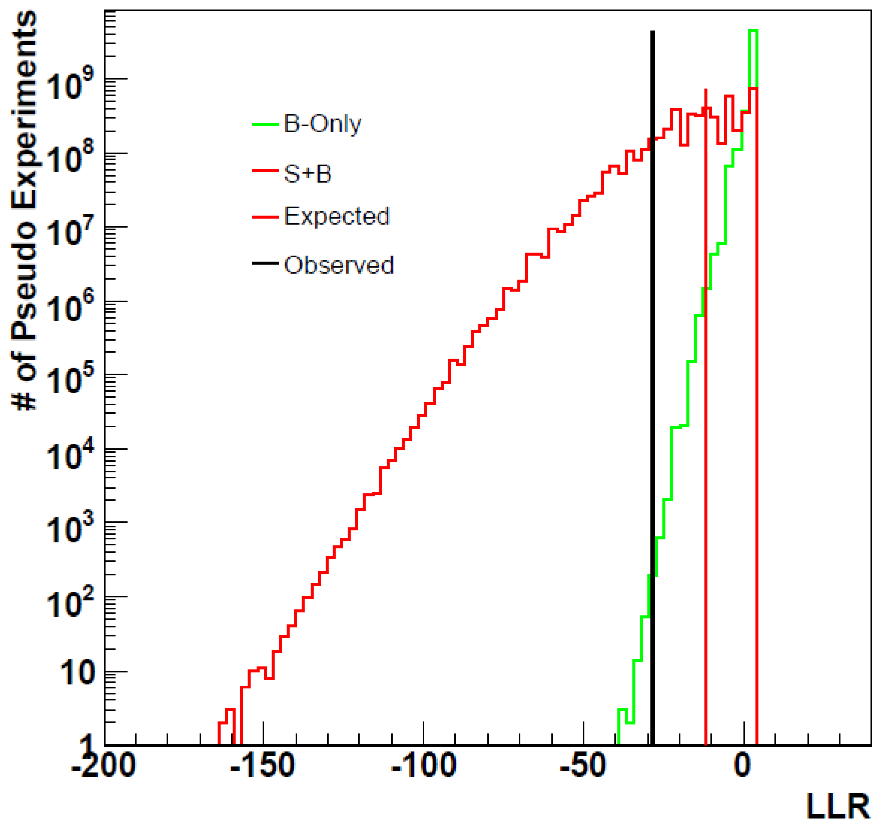

- Probability for signal plus background to give less signal-like observations than the observed one is 0.87

Combination with other ZZ results

- Use same LLR test statistic
- Combination of the 4*l* analyses:
  - PRL 100, 131801 (2008)
  - p-value of 2.9 x 10^{-7}
  - 5.0σ (4.2σ expected)
- Combination of above with 2*l*2ν analysis:
  - Published PRD 78, 072002 (2008)
  - p-value of 6.2 x 10^{-9}
  - 5.7σ (4.8σ expected)

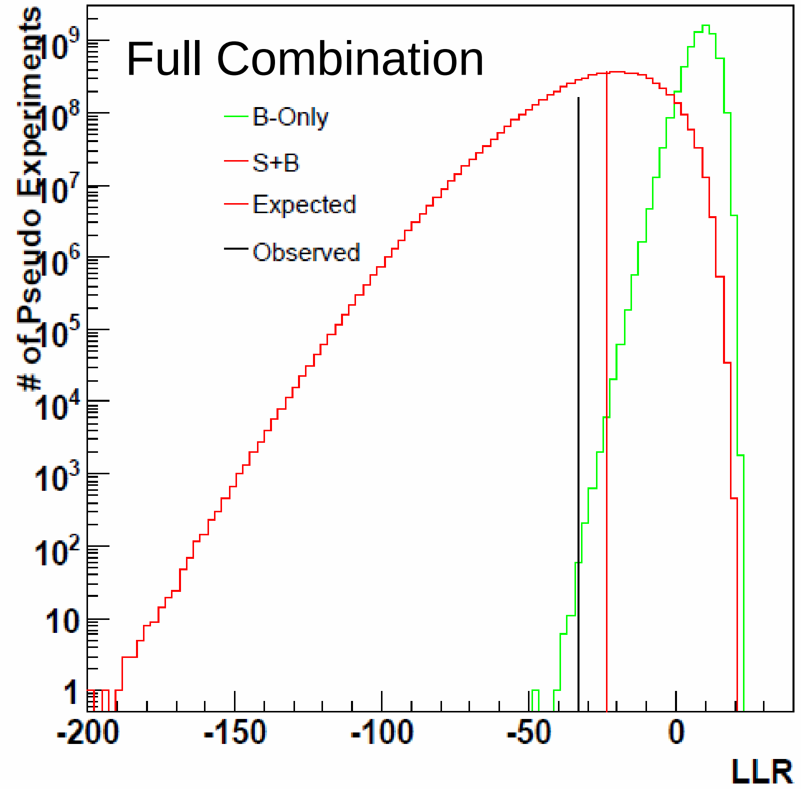

- Probability for signal plus background to give less signal-like observations than the observed one is 0.71

Results

- Minimize a fit to the systematic parameters in the LLR leaving the signal rate as a free parameter to extract the cross-section:

$$\sigma(ZZ) = 1.60 \pm 0.63\ (\text{stat.})^{+0.16}_{-0.17}\ (\text{syst.})\ \text{pb}$$

- SM prediction: 1.4 ± 0.1 pb

- Published PRL 101, 171803 (2008)

Results cont'd

- Look for ZZ combining three channels: $2l2\nu$ and $4l$ (two running periods)
- Combination of analyses results in an observation with significance of 5.7σ
- Cross section of combination is consistent with standard model expectation and in very good agreement with value measured by CDF: $\sigma(ZZ) = 1.4^{+0.7}_{-0.6}$ pb

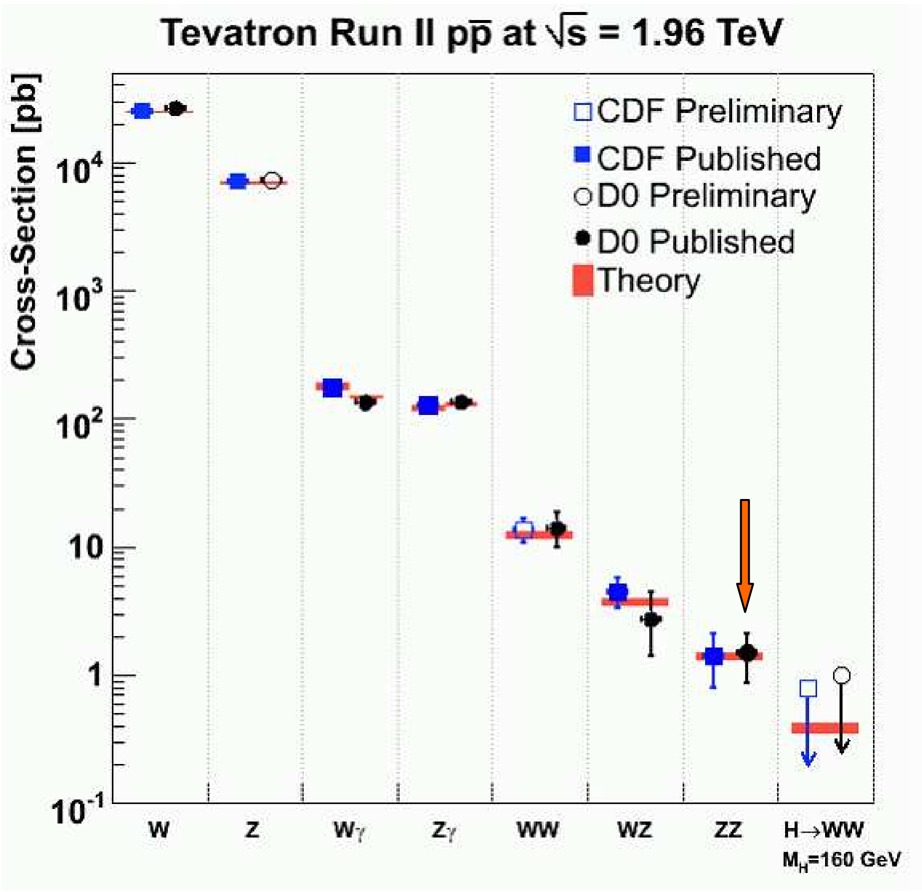

H→WW points not yet updated

Measuring ZZ Anomalous Couplings

- Evidence of non-zero coupling would be reflected by increased cross-sections.
- Currently setting limit on anomalous couplings in the *ZZ* channel using the same *ZZ* to 4 lepton data set since there was no excess
- Excursions from SM for ZZ case can be described via an effective Lagrangian which preserves Lorentz invariance and U(1) gauge invarience:

$$L = \sum_{V=Z,\gamma} -\frac{e}{M_Z^2}\left[f_4^V (\partial_\mu V^{\mu\beta}) Z_\alpha (\partial^\alpha Z_\beta) + f_5^V (\partial^\sigma V_{\sigma\mu}) \tilde{Z}^{\mu\beta} Z_\beta \right]$$

where $V_{\mu\nu} = \partial_\mu V_\nu - \partial_\nu V_\mu$ and $\tilde{Z}^{\mu\beta} = \frac{1}{2}\varepsilon_{\mu\beta\rho\sigma} Z^{\rho\sigma}$

- f_4^V and f_5^V are predicted to be 0 at tree level
- Unitarity violation is avoided by introducing a form-factor scale Λ, modifying the anomalous coupling at high energy: $f_i^V(\hat{s}) = \frac{f_i^V(0)}{(1+\hat{s}/\Lambda^2)^n}$

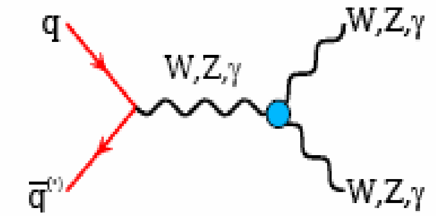

$q\bar{q}' \to W^{(*)} \to W\gamma$: $WW\gamma$ only

$q\bar{q}' \to W^{(*)} \to WZ$: WWZ only

$q\bar{q} \to Z/\gamma^{(*)} \to WW$: $WW\gamma, WWZ$

$q\bar{q} \to Z/\gamma^{(*)} \to Z\gamma$: $ZZ\gamma, Z\gamma\gamma$

$q\bar{q} \to Z/\gamma^{(*)} \to ZZ$: $ZZ\gamma, ZZZ$

Absent in SM

- Compare number of observed events to expected background from a MC that allows for non-zero couplings

U. Baur, D. Rainwater, “Probing neutral gauge boson self-interactions in ZZ production at hadron colliders”, Phys. Rev. D 62, 113001 (2000).

Conclusion

- I've had varied experience on two collaborations
  - Experience with hardware assembly, installation, commissioning and operation
  - Experience with setting up a framework for validation of simulated and real data
  - Experience in analysis using large datasets available only at Tevatron
- I'm excited to have been able to do my work at what is currently the highest energy collider, and think there is still time for many new, exciting measurements before publications start coming from the LHC
- I think working as a Research Associate at Fermilab would allow me to continue helping the lab achieve its physics results as well as continue giving me the experience needed to eventually get a faculty position

Backup

Regge Theory

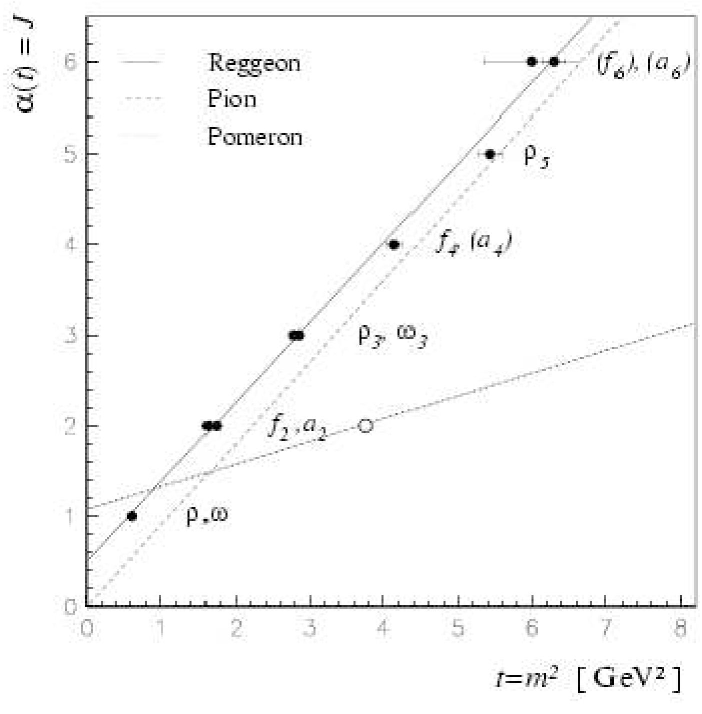

- Interprets strong interactions as proceeding via exchange of particle trajectories $\alpha(t)$ where $\alpha(t)$ is a complex function of angular momentum
- Particles are organized in sequences with increasing mass (m) and spin (J) represented by resonances in the amplitude of the exchange in the t-channel which is proportional to: $\frac{1}{l - \alpha(t)}$ where l is the angular momentum.
- Resonances form Regge poles corresponding to the exchange of particles were $\alpha(m) = J$.

Ingelman-Schlein Model

- Attempt to blend Regge theory with perturbative QCD

- Factorize the cross section

$$\frac{d^2\sigma(p+\overline{p}\to\overline{p}+X)}{d\xi dt} = F_{I\!P/\overline{p}}(\xi,t)\sigma(I\!P+p\to X)$$

- Flux factor given by a global fit found by Donnachie and Landshoff and remaining part of cross section can be factorized leaving as the only unknown the structure function of the Pomeron (proposed as two quarks or two gluons of flavor similar to proton)

- Hard scattering probes structure of Pomeron (jet production --> gluon structure, W production --> quark structure)

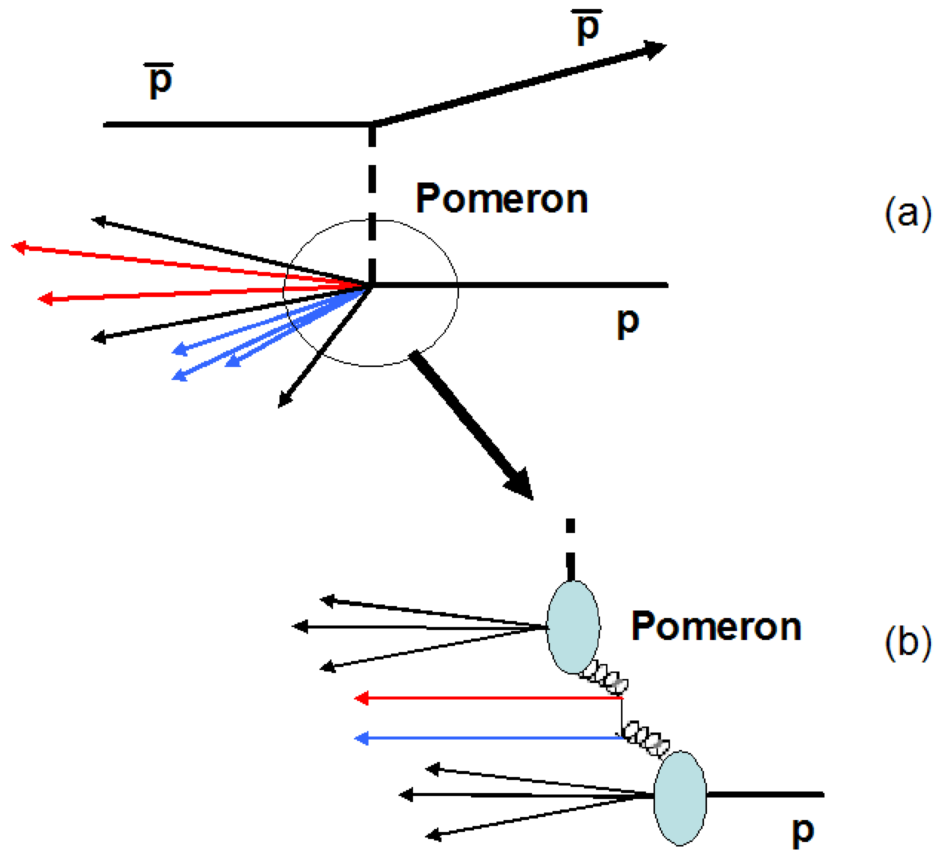

G. Ingelman and P. Schlein, Phys. Lett. **B** 152, 256 (1985)

BFKL Model

- Proposes a more involved gluon structure for the Pomeron
- Add perturbative corrections to two reggeized gluons to form a gluon ladder

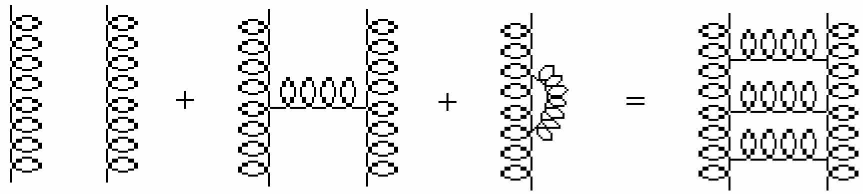

- Use leading logarithmic approximation as the resummation scheme following the BFKL equation
- Resummed amplitude has a cut in the complex angular momentum plane called the BFKL Pomeron
- Causes a different jet topology than DGLAP

L.N. Lipatov, Sov. J. Nucl. Phys. **23**, 338 (1976); E.A. Kuraev, L.N. Lipatov and V.S. Fadin, Sov. Phys. JETP **44**, 443 (1976); Sov. Phys. JETP **45**, 199 (1977); Y.Y. Balitsky and L.N. Lipatov, Sov. J. Nucl. Phys. **28**, 822 (1978)

Soft Color Evaporation

- Account for rapidity gaps without need of a Pomeron

- Allow soft color interactions to change the hadronization process such that color lines are canceled and rapidity gaps appear (non-perturbative, color topology of event changes)

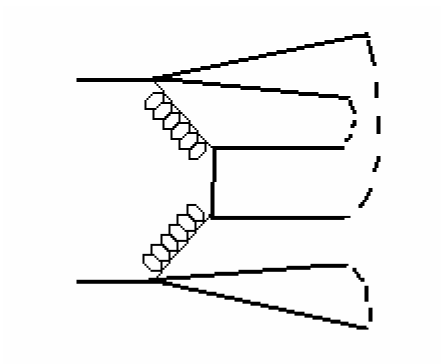

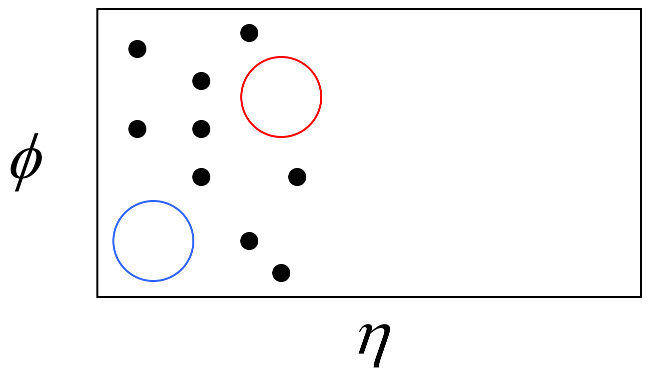

- Look at difference in gap production of gluon processes vs. quark processes to find evidence

R. Enberg, G. Ingelman, and N. Timneanu, Phys. Rev. D **64**, 114015 (2001).

DØ Coordinate System

- Right-handed Cartesian coordinate system:
  - +z in direction of proton beam around the ring
  - +y vertically upwards
  - +x perpendicular to y away from center of the ring
- Cylindrical-Polar coordinate system:
  - r is the radial distance from the z-axis
  - ϕ is the azimuthal angle with $\phi = 0$ along the +x-axis
  - θ is the polar angle with $\theta = 0$ is in the positive z direction
- Lorentz-invariant variables:
  - Transverse Energy: $E_T = E \sin \theta$
  - Transverse Momentum: $p_T = \sqrt{p_x^2 + p_y^2}$
  - ϕ
- Additional variables:
  - Rapidity: $y = \frac{1}{2}\log\left(\frac{E+p_z}{E-p_z}\right) \longrightarrow \eta = -\ln\left(\tan\left(\frac{\theta}{2}\right)\right)$ (for $E >> m$)
- Variables can be expressed relative to the IP (physics) or z = 0 (detector)

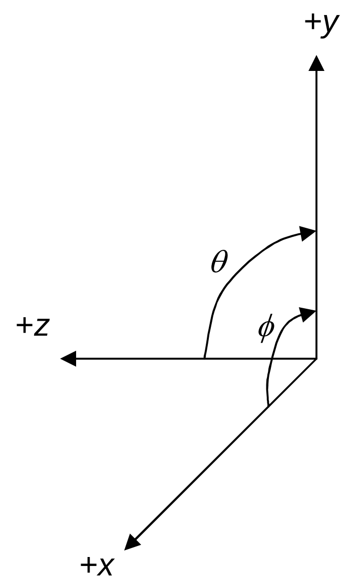

Detector Needs

- Position resolution of 100µm
  - Dictated by a comparable uncertainty in beam position
- High efficiency
- Modest radiation hardness
  - 0.03 MRad yearly dose expected
- High rate capability
  - Active at every beam crossing
- High background rejection
  - Insensitive to particles away from the active area showering along beam pipe
- Small dead area close to the beam
  - Protons are scattered at very low angles, acceptance is very dependent on position relative to beam
- Scintillating Fiber detector spliced with waveguide fibers meets these needs

FPD Fiber Preparation

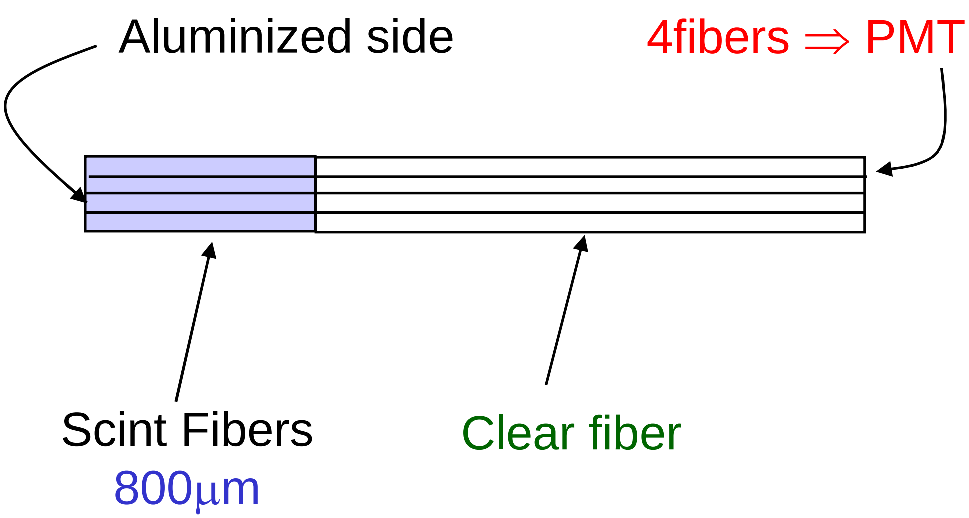

- Scintillating fibers emit in the blue part of the spectrum with a peak emission wavelength of about 475nm and providing around 10 detected scintillation photons from a typical particle
- Fibers are polished using an ice polishing method
- Scintillating fibers are spliced to clear fibers using an intense light beam that fuses the fibers together and provides for over 90% transfer of light through the splice point
  - Light output is improved due to longer attenuation length of the clear fiber
  - Cross talk is reduced

FPD Readout

- Light from the fibers in a channel is detected by a pixel of the MAPMT
- The cookie is held against the face of the MAPMT
  - The provides for a measure of cross-talk between the channels at the level of around 2.5% for ideal alignment, up to 10% if alignment is off
- 7 MAPMTs and one Trigger PMT are housed in a cartridge top which fits over the cartridge base and holds the tubes in alignment with the fibers
- Signals are conveyed to Amplifier/Shaper boards in the tunnel and then to the central DØ readout electronics

(a) (b)

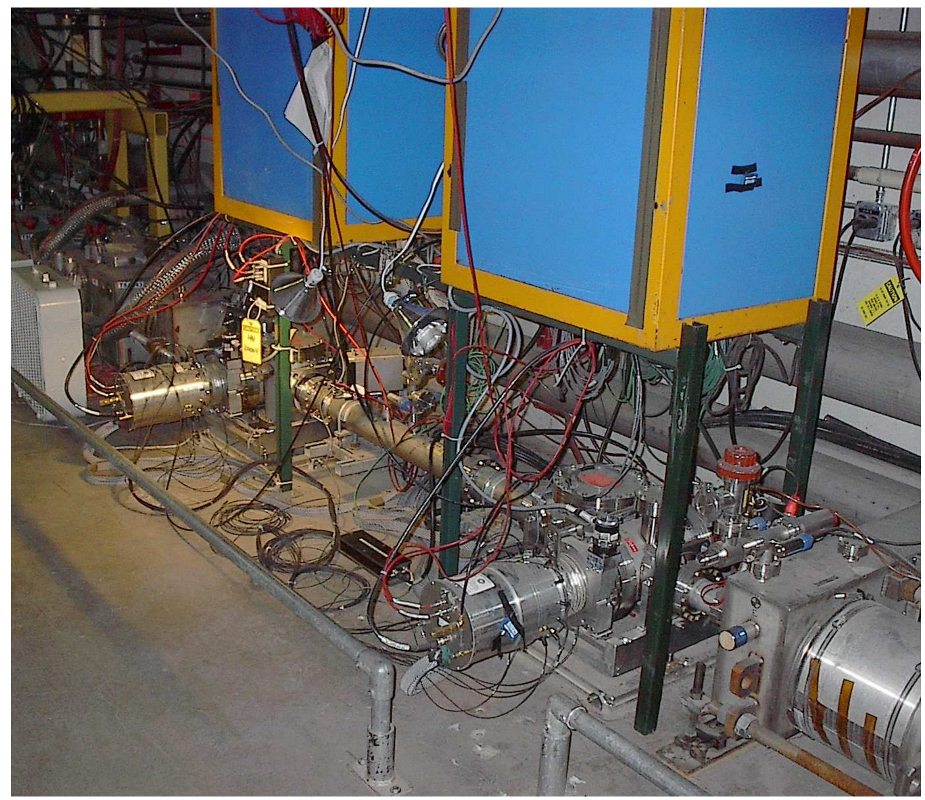

FPD Operations

- The pots need to be operated near the beam (~10-20mm), yet need to be moved transversely away from the beam at the end of store and during beam injection.
- The motion system consists of a step motor and a set of reduction gears resulting in movement with a precision of approximately 8 μm per half turn of the motor. Position is also monitored with a linear variable differential transformer (LVDT) with the values used for the safety system.
- The system is monitored and controlled through a python program, which sends commands to the electronics in the tunnel. The pots are able to move at fast (6-8mm / minute) or slow (1-2mm / minute) speeds.
- Rates from the trigger tubes are monitored to verify how the pots are interacting with the beam halo and to provide information for the safety system.
- Power to the system is controlled through a switch in the DØ control room

FPD Operating Positions

- At each pot location, there is a "sigma" value associated with the beam profile in the x and y directions, σ_x and σ_y respectively.
- Positions are determined for each pot based on singles rates and halo effects (distance from home, home ~45mm from beam)
- Operating positions are determined for each spectrometer where pots are at matched sigma positions
- Multiple positions are provided to help account for changes in beam conditions between stores

			1-Feb-05				
			Dipoles				
I sigma	15.4		13.4		12.4		11.4
D1I	30.50	31.27	32.05	32.44	32.82	33.21	33.60
D2I	27.88	28.58	29.29	29.64	29.99	30.34	30.69
			A Vertical				
U sigma	14.6		12.6		11.6		10.6
A1U	26.45	27.49	28.52	29.04	29.56	30.08	30.60
A2U	30.12	30.93	31.73	32.14	32.54	32.94	33.35
A1D	30.97	32.01	33.04	33.56	34.08	34.60	35.11
A2D	32.22	33.03	33.83	34.23	34.64	35.04	35.44
D sigma	14.2		12.2		11.2		10.2
			A Horizontal				
I sigma	15.9		13.9		12.9		11.9
A1I	11.14	12.97	14.81	15.72	16.64	17.56	18.48
A2I	14.74	16.28	17.83	18.60	19.37	20.14	20.91
A1O	16.09	17.92	19.75	20.67	21.59	22.50	23.42
A2O	21.82	23.36	24.90	25.67	26.44	27.21	27.98
O sigma	16.0		14.0		13.0		12.0
			P Vertical				
U sigma	12.8		10.8		9.8		8.8
P1U	20.66	22.52	24.37	25.30	26.23	27.15	28.08
P2U	23.87	25.42	26.97	27.74	28.52	29.29	30.07
P1D	18.54	20.39	22.25	23.18	24.10	25.03	25.96
P2D	21.22	22.77	24.33	25.10	25.88	26.65	27.43
D sigma	12.9		10.9		9.9		8.9
			P Horizontal				
I sigma	17.3		15.3		14.3		13.3
P1I	26.48	27.50	28.53	29.04	29.55	30.06	30.57
P2I	29.31	30.11	30.92	31.32	31.72	32.12	32.52
P1O	24.32	25.34	26.36	26.87	27.38	27.90	28.41
P2O	30.48	31.29	32.09	32.49	32.89	33.29	33.69
O sigma	17.5		15.5		14.5		13.5

Proton Reconstruction

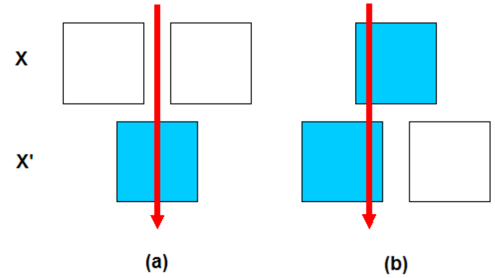

- Combinations of fibers in a plane determine a segment

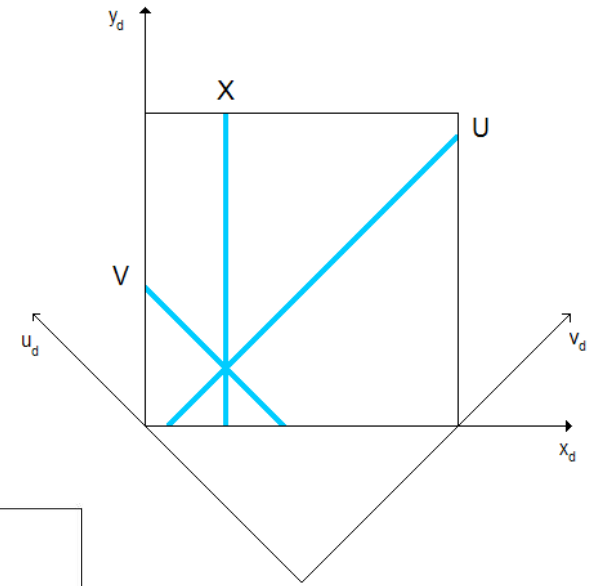

- Need minimum of two out of three segments to get a hit
  - u/v, u/x, x/v (or u/x/v)
    - Can reconstruct an x_d and y_d

- Validated hits require all three segments within hit resolution agreement ($|x\_uv – x\_x| < 4\sigma$)
  - Theoretical hit resolution from size of segments is 78μm

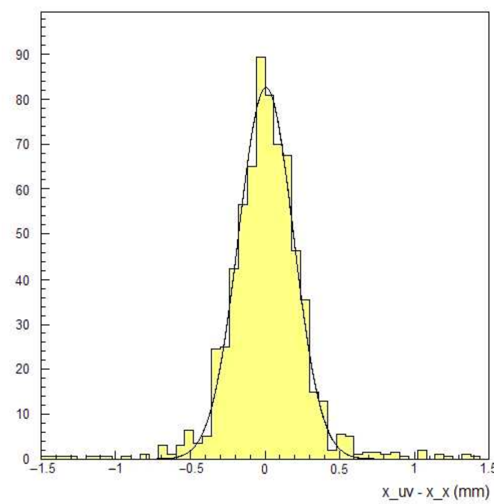

- Require a validated hit in both detectors of spectrometer

Jet Reconstruction

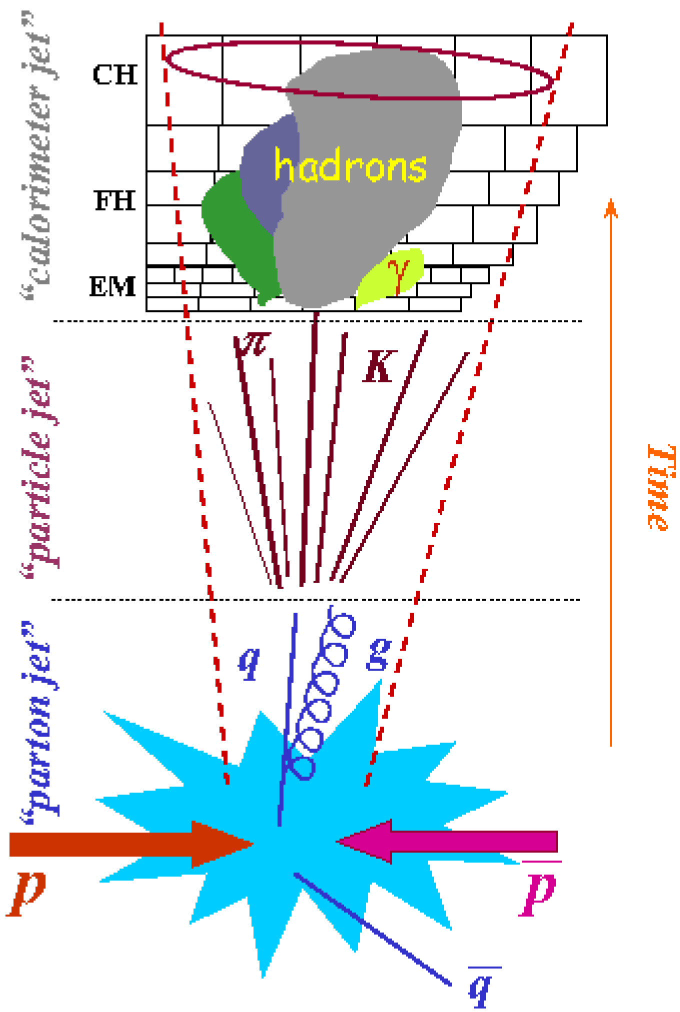

- In addition to protons from the FPD, this analysis requires jet reconstruction
- Energy deposited in the calorimeter comes from sprays of particles lying along the direction of a parton from the hard interaction
- Jet algorithms are employed to combine the appropriate detector data into the jet such that the properties of a calorimeter jet are correlated with those of a parton jet so comparisons to theory can be made
- Jets are corrected for an overall energy scale which associates measured energy with particle jets

Improved Legacy Cone Algorithm

- The algorithm used at DØ is a cone algorithm
  - i.e. a geometric definition of a jet where energy within a cone of some size $R = \sqrt{\Delta\phi^2 + \Delta\eta^2}$ (for this analysis, R = 0.7) is considered to be a jet
- Detector jets are formed from calorimeter towers. Cells of sufficient energy that are not considered "hot" are included in the recombination. This schemes uses 4-momenta:

$$P^{\mu}_{tower} \equiv (E_{tower}, \mathrm{p}_{tower}) = \sum_{cell} P^{\mu}_{cell}$$

$$P^{\mu}_{jet} \equiv (E_{jet}, \mathrm{p}_{jet}) = \sum_{tower} P^{\mu}_{tower}$$

- Only towers within the cone radius are considered
- Iterative procedure

Fiber Correlations

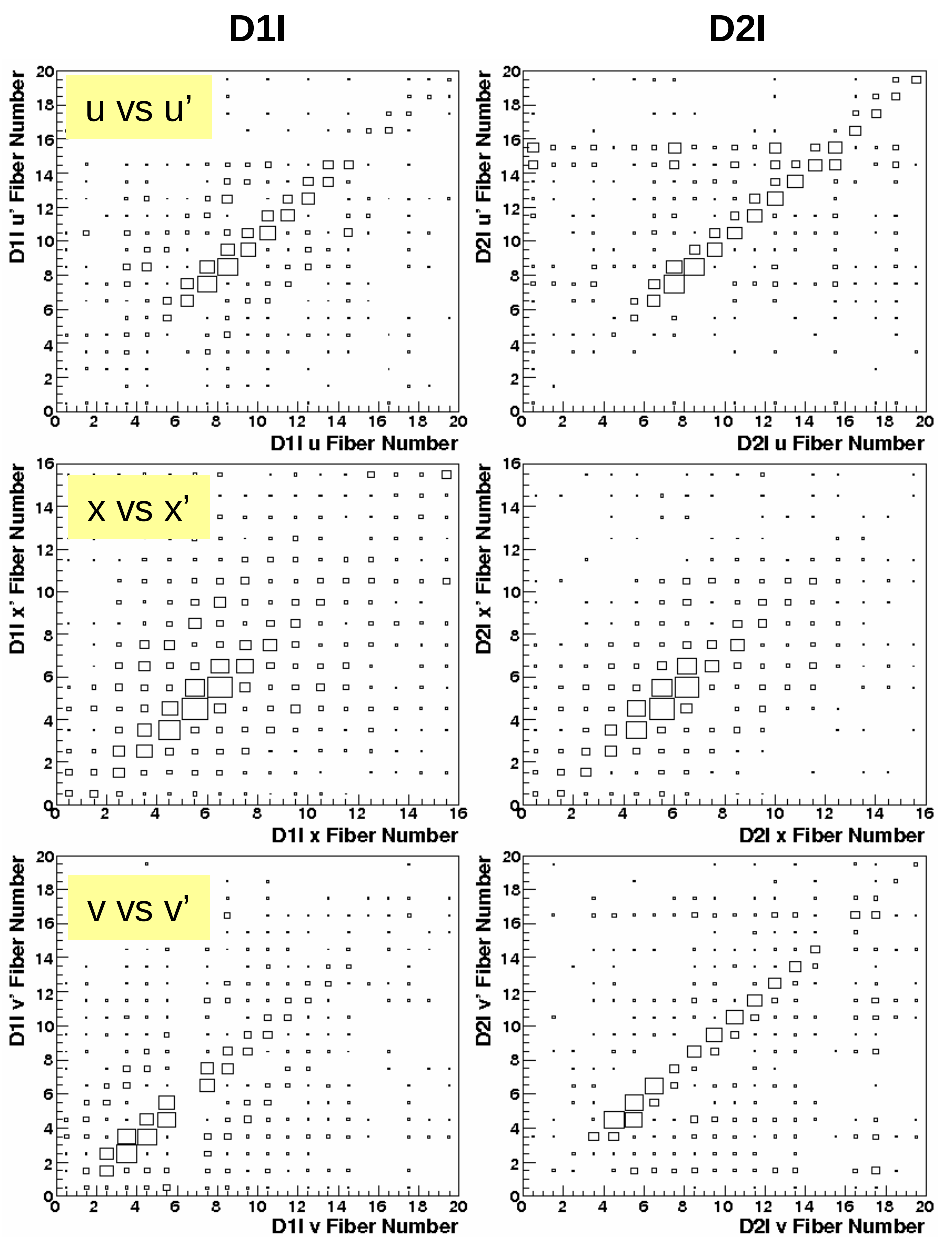

- Correlations between fibers of layers within a plane from events with multiple segments but only one validated hit per detector (prototrack or halo)
- Can clearly see the expected correlation between fibers indicating the passage of particles through the frame firing fibers in both layers.

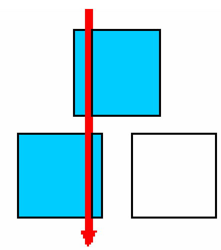

- The loose segment requirement also introduces “noise” fibers and some MAPMT cross-talk is also apparent
- The noise is removed in next step of reconstruction (better optimization of the discrimination could also remove this)

Hit Resolution and Hit Map

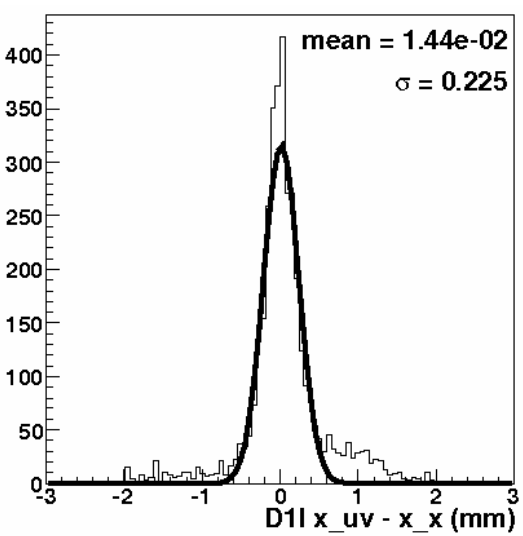

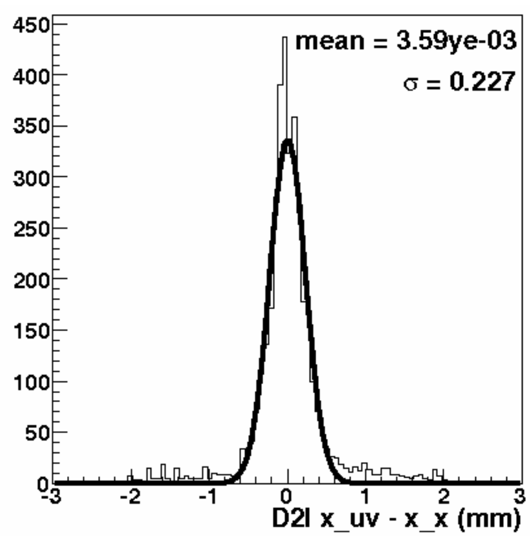

- Hit resolution (after mapping correction) gives:
  - 159μm for D1I
  - 160μm for D2I
- Hit maps for validated hits (independent for each detector) fills out the detector showing the expected edges

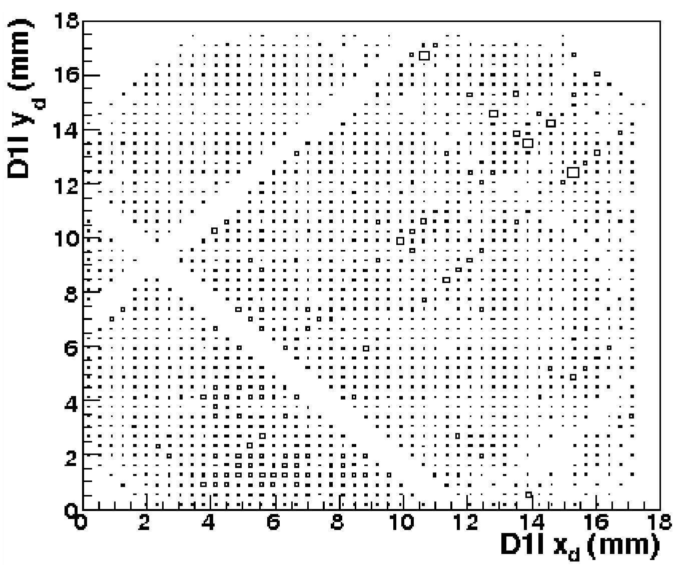

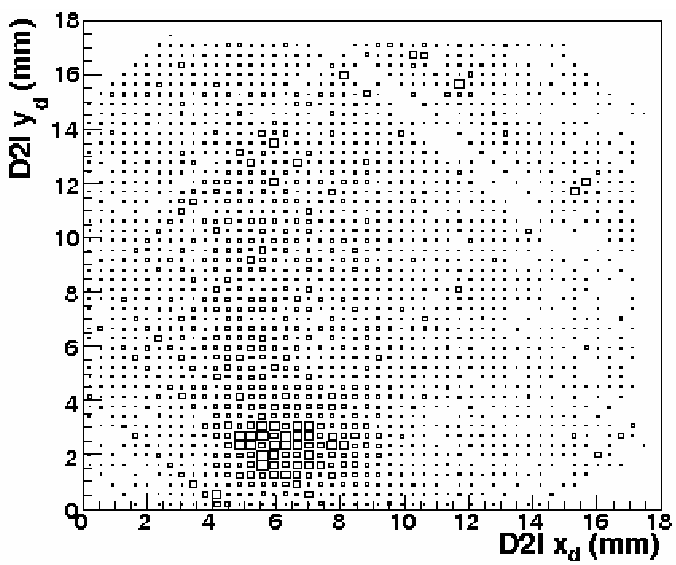

Data Merging

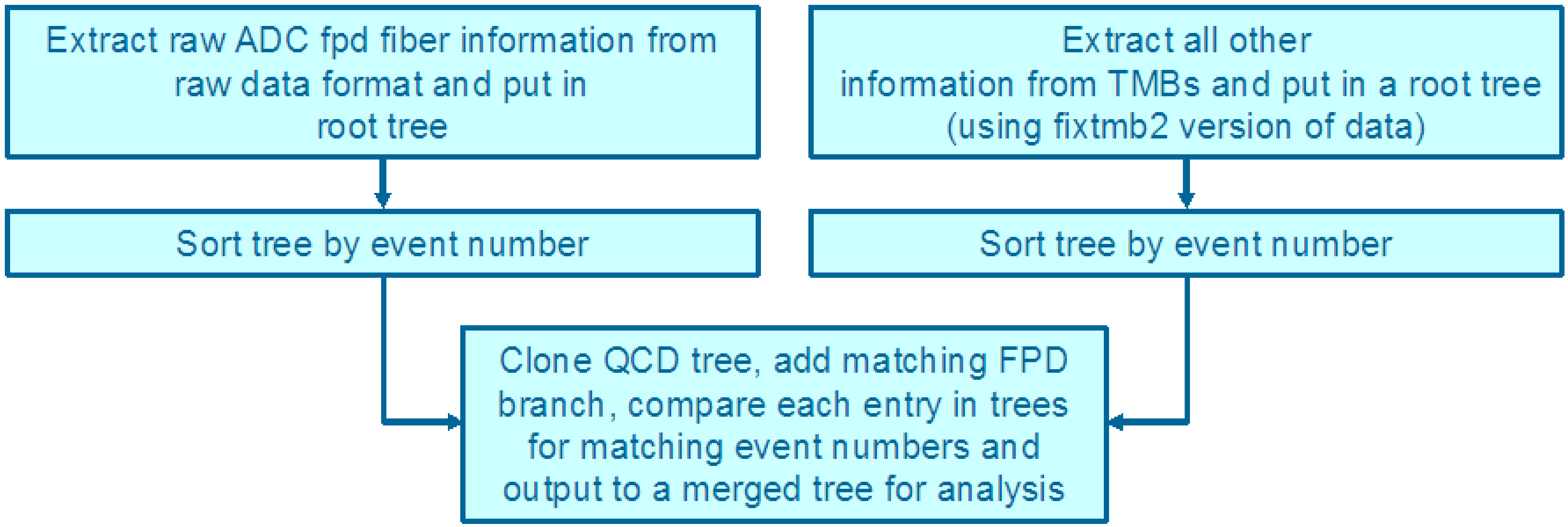

- Since data existed in two independent datasets, it was necessary to merge the two sample together in order to perform an analysis including both the FPD and the central DØ information.
- The data was extracted from each dataset on a run-by-run basis with resulting information in root-tree format
- Each run was sorted by event number, then the two sample were merged into the final analysis tree
- The FPD data is reconstructed on an event-by-event basis as the data is being analyzed

Global

- Uses minbias events generated in Pythia for validation sample
  - Also run automatically with all other MC samples
- Uses full magnetic field and looks at values in all sub-detectors simultaneously in global coordinates
- Hits
  - Looks at generator vertex and tracks
  - Keeps track of positions, times of flight and energy of hits
  - Currently uses χ^2 test
- Digis
  - Looks at digitized values for hits and energy deposition
- Reco
  - Looks at digitized values processed through the reco code, compared to hit level results

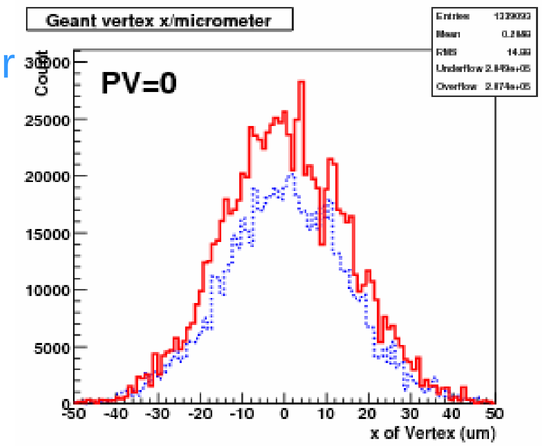

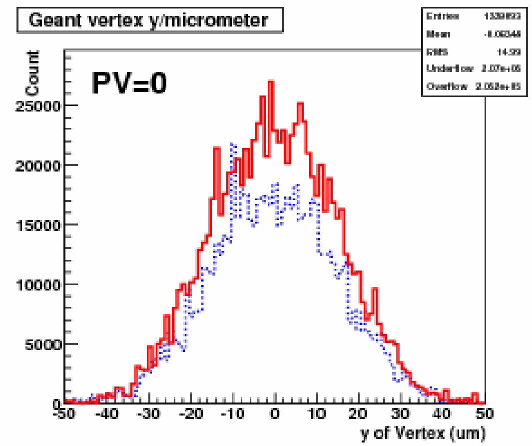

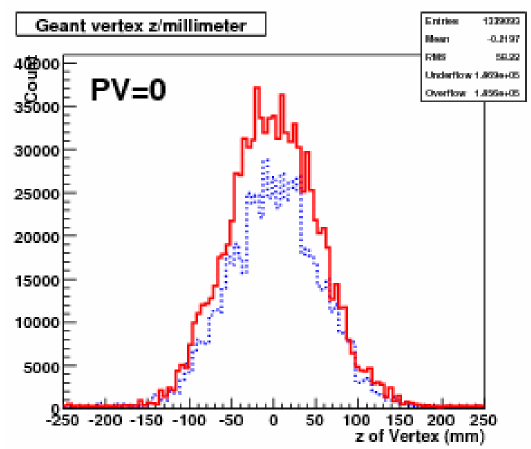

Example of looking at different sized samples

Example Global Plots

- Example of plots for Hcal
  - From QCD pt 50-80 RelVal sample
- Digi plot shows analog equivalent energy
- Rechit plots shows resolution between reconstructed energy and simhit energy

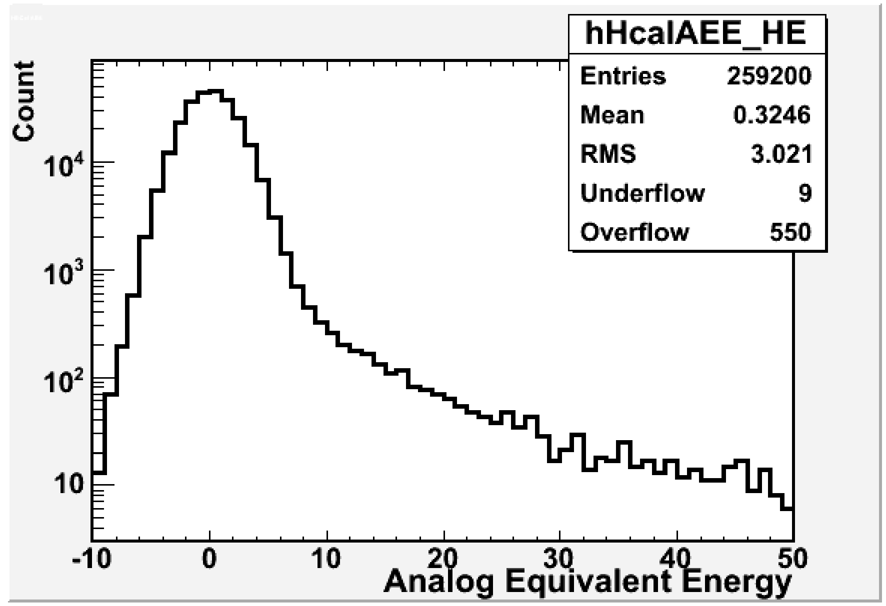

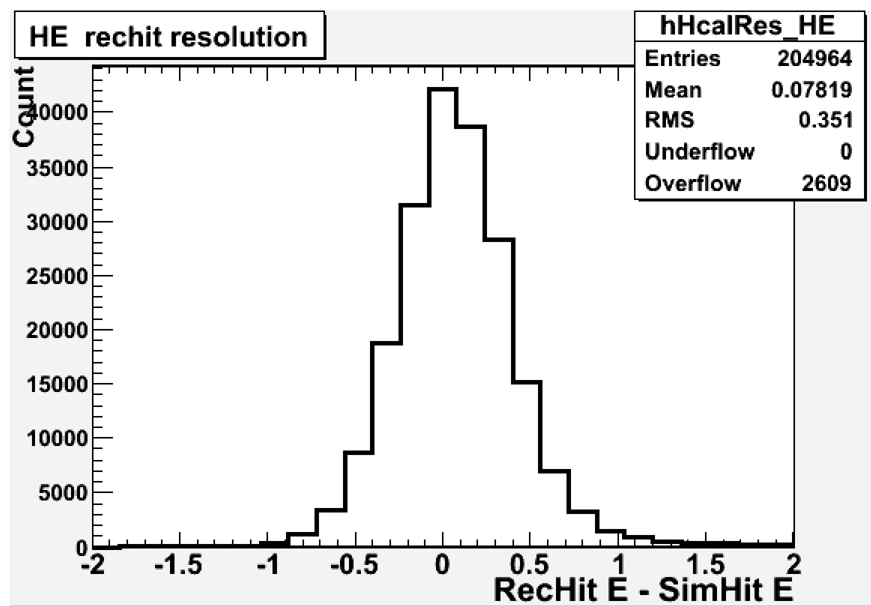

First DØ ZZ Analysis

- Looked at 4e, 4μ and 2e2μ channels
- Required a dilepton mass cut of 30 GeV
- Observe one $ee\mu\mu$ candidate in 1 fb^{-1} of data
  - Expected background of 0.13 ± 0.03 vents
  - SM predicts 1.71 ± 0.15 events
    - M(ee) = 93.4 GeV
    - M(μμ) = 33.4 GeV
- Set upper limit of $\sigma(ZZ/Z\gamma^*)$ < 4.4 pb at 95% CL
- Set Limits on Anomalous Couplings

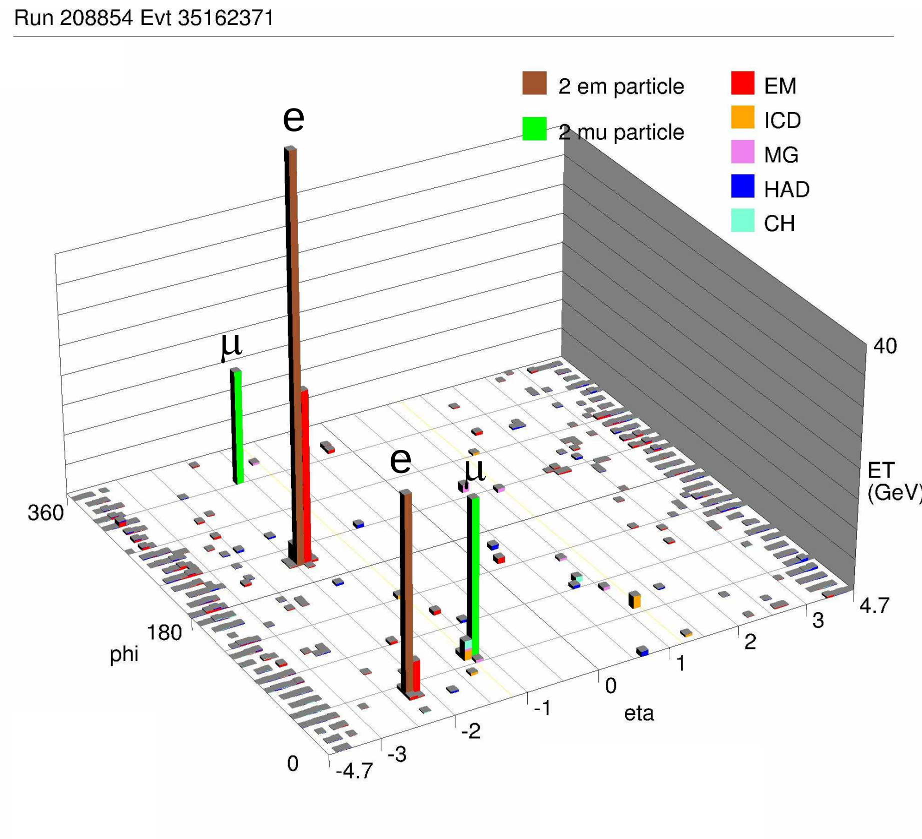

PRL 100, 131801 (2008)

Limits on anomalous ZZZ^* and $ZZ\gamma^*$ couplings

- ZZ channel sensitive to two couplings
- 95% CL limits on anomalous couplings for Λ = 1.2 TeV

$$-0.28 < f_{40}^{Z} < 0.28$$

$$-0.31 < f_{50}^{Z} < 0.29$$

$$-0.26 < f_{40}^{\gamma} < 0.26$$

$$-0.30 < f_{50}^{\gamma} < 0.28$$

- First bounds on these limits from Tevatron
- f_{40}^{Z}, f_{50}^{Z}, f_{50}^{γ} are most restrictive to date

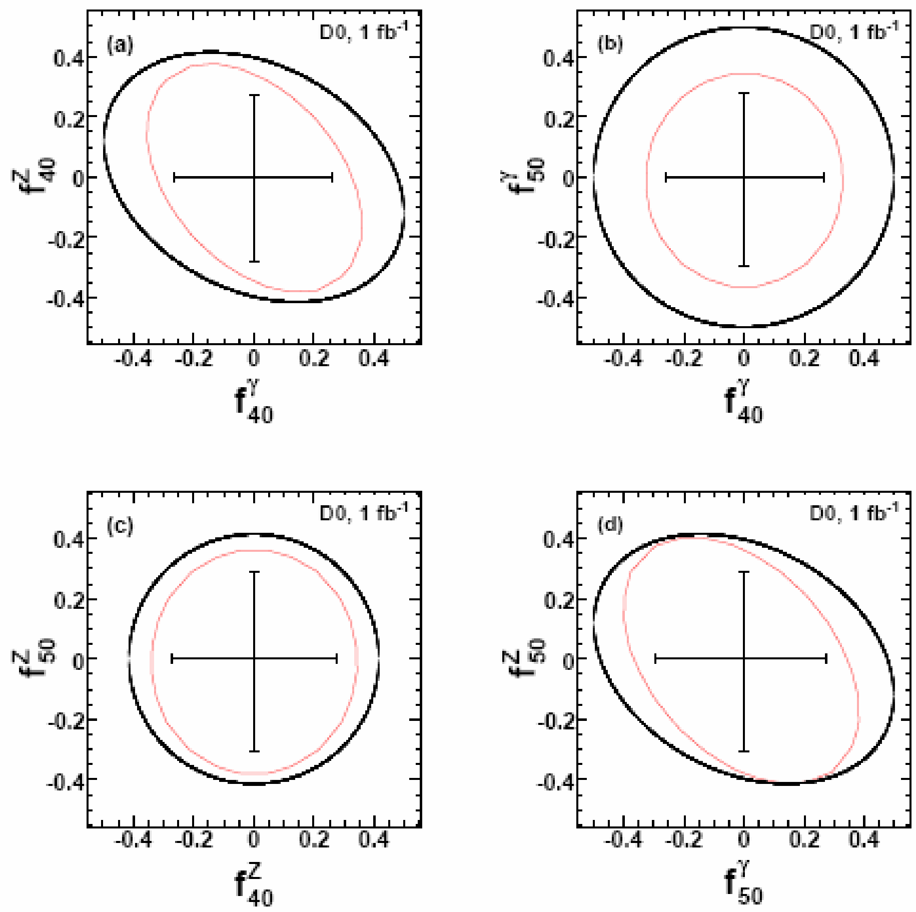

CDF $ZZ \rightarrow llll$

- Split 4e, 4μ and 2e2μ into 7 exclusive categories depending whether a lepton has a track and/or is identified explicitly
- One pair of leptons with M(*ll*) in [76 – 106] GeV; the other pair with M(*ll*) in [40 – 140] GeV

$1\ \text{fb}^{-1}$ Category	Candidates without a a trackless electron	Candidates with a a trackless electron
ZZ	$1.990 \pm 0.013 \pm 0.210$	$0.278 \pm 0.005 \pm 0.029$
Z+jets/Zγ+jets	$0.014^{+0.010}_{-0.007} \pm 0.003$	$0.082^{+0.089}_{-0.060} \pm 0.016$
Total	$2.004^{+0.016}_{-0.015} \pm 0.210$	$0.360^{+0.089}_{-0.060} \pm 0.033$
Observed	**2**	**1**

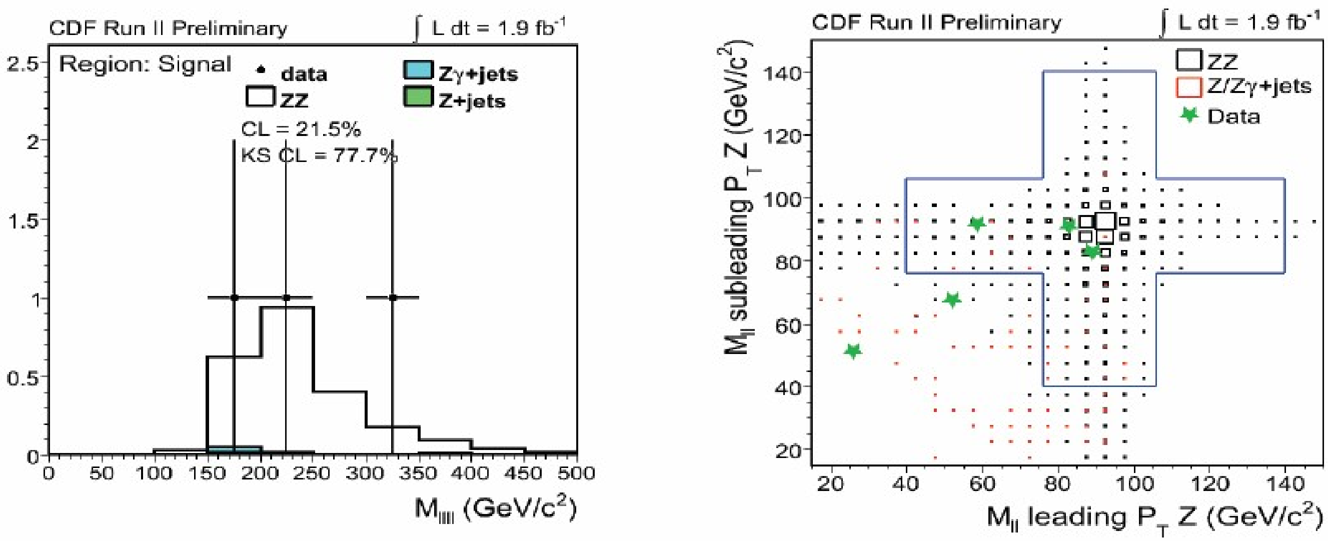

CDF $ZZ \rightarrow ll\nu\nu$ and Combination

- Select events with $ee/\mu\mu$ and large MET. Veto on central jets to suppress ttbar contribution.
  - Observe 276 events in preselected sample
  - Expect 14 ± 2 signal events
- Use full kinematic information to form a likelihood ratio

$$LR \equiv \frac{P_{ZZ}}{P_{ZZ} + P_{WW}}$$

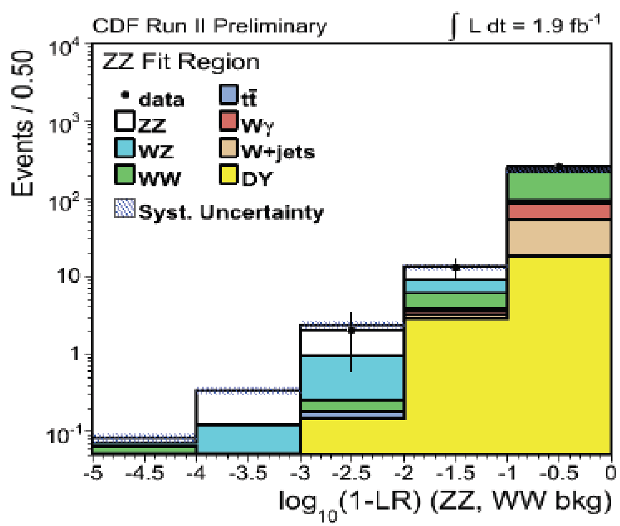

- Combine $ZZ \rightarrow llll$ and $ZZ \rightarrow ll\nu\nu$ channels:

50% chance to observe 5σ effect

Observed Results

P-Value	0.12	1.1×10^{-5}	5.1×10^{-6}
Significance	$1.2\ \sigma$	$4.2\ \sigma$	$4.4\ \sigma$

- Cross section measurement:

$$\sigma(ZZ) = 1.4^{+0.7}_{-0.6}\ \mathrm{pb}$$

PRL 100, 201801 (2008)

$ZZ \rightarrow ll\nu\nu$: ee Results

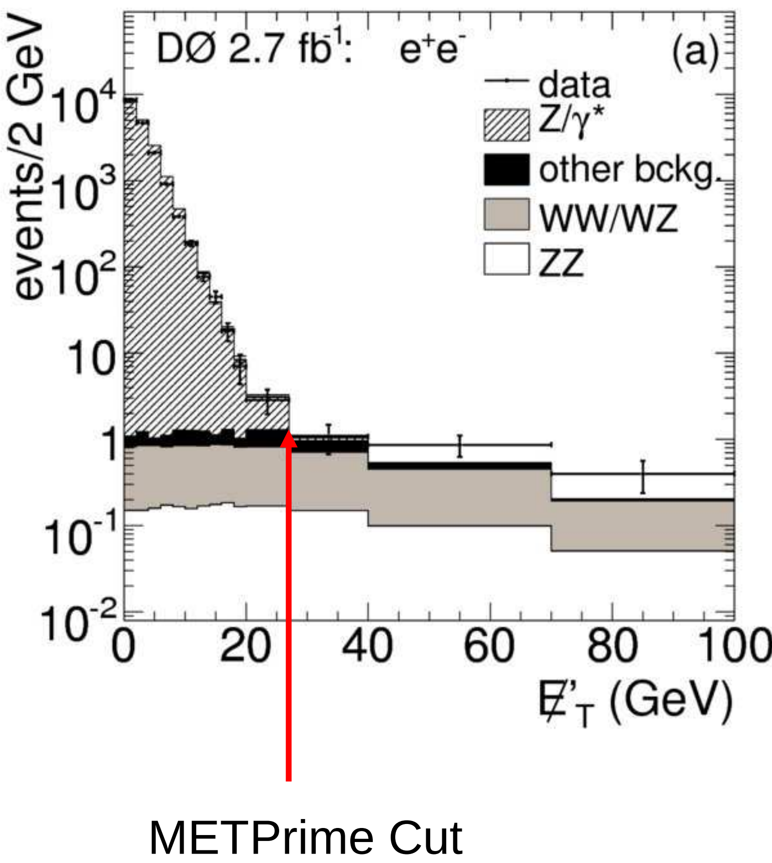

Sample	dilepton selection	$\not{E}'_T$ requirement
$Z \to \ell^+\ell^-$	1.18×10^5	0.5 ± 0.2
$Z \to \tau^+\tau^-$	48.3	0.35
W+Jets	18.2	2.7 ± 0.4
$t\bar{t}$	16.4	0.34
WW	28.0	10.6 ± 0.1
WZ	19.2	1.08
$W\gamma$	2.0	0.01
Predicted Background	1.19×10^5	15.6 ± 0.4
$ZZ \to \ell^+\ell^-\ell'^+\ell'^-$	2.9	0.02
$ZZ \to \ell^+\ell^-\nu\bar{\nu}$	8.9	4.03
Predicted Total	1.19×10^5	19.6 ± 0.4
Data	118,850	28

ZZ→*ll*νν: μμ Results

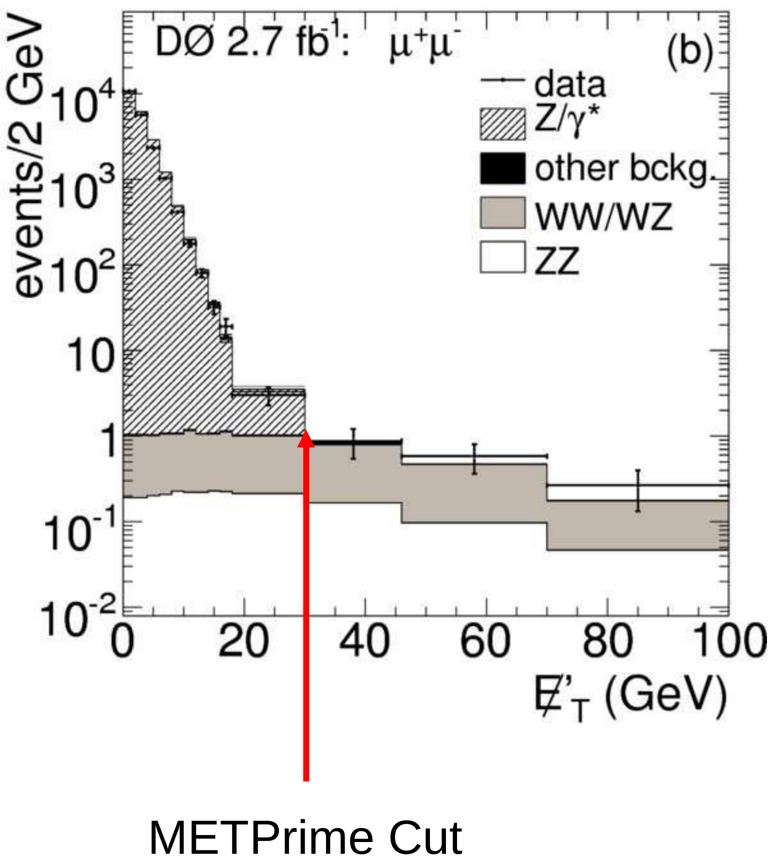

Sample	dilepton selection	$\not\!\!E'_T$ requirement
$Z \to \ell^+\ell^-$	1.30×10^5	0.1 ± 0.1
$Z \to \tau^+\tau^-$	53.3	0.09
W+Jets	–	< 0.01
$t\bar{t}$	16.0	0.21
WW	32.0	9.7 ± 0.1
WZ	18.3	0.82
Predicted Background	1.30×10^5	10.9 ± 0.3
$ZZ \to \ell^+\ell^-\ell'^+\ell'^-$	2.89	0.00
$ZZ \to \ell^+\ell^-\nu\bar{\nu}$	9.48	3.39
Predicted Total	1.30×10^5	14.3 ± 0.3
Data	127,960	15

RunIIa 4*l* result

- For combination, need to scale signal and background expectation to new mass cut and we also lose the candidate event
  - Use MC samples from current analyses
  - Use mass and pT requirements from earlier analysis
  - Remove extra isolation requirements on muons
  - Repeat only changing the mass requirement to new values
  - Determine a scale factor applied expected signal and background from previous analysis and add the three channels into the LLR calculation

- A 3% systematic uncertainty is applied due to the rescaling

Shared Systematics

- Correlated
  - Lepton resolution
  - ZZ p_T spectrum
    - Account for higher order corrections on signal acceptance
  - PDF uncertainties

- Uncorrelated
  - Electron misidentification
    - Determined using different methods
  - Multihadron sample statistics
    - Regions of phase-space are different